DIP-COATING OF CALCIUM HYDROXYAPATITE ON TITANIUM ALLOY (Ti-6Al-4V) AND STAINLESS STEEL (316L) SUBSTRATES

A THESIS SUBMITTED TO
THE GRADUATE SCHOOL OF NATURAL AND APPLIED SCIENCES
OF
THE MIDDLE EAST TECHNICAL UNIVERSITY

BY

BORA MAVİŞ

IN PARTIAL FULFILLMENT OF THE REQUIREMENTS FOR

THE DEGREE OF MASTER OF SCIENCE

IN

THE DEPARTMENT OF METALLURGICAL AND MATERIALS

ENGINEERING

JANUARY 1999

Approval of the Graduate School of Natural and Applied Sciences

Prof. Dr. Tayfur ÖZTÜRK
Director

I certify that this thesis satisfies all the requirements as a thesis for the degree of Master of Science.

Prof. Dr. Naci SEVİNÇ
Head of Department

This is to certify that I have read this thesis and that in my opinion it is fully adequate, in scope and quality, as a thesis for the degree of Master of Science.

Assoc. Prof. Dr. A. Cüneyt TAŞ
Supervisor

Examining Committee Members

Prof. Dr. Mustafa DORUK (Chairman)

Prof. Dr. Meral KIZILYALLI

Prof. Dr. Ahmet GEVECİ

Assoc. Prof. Dr. Bilgehan ÖGEL

Assoc. Prof. Dr. A. Cüneyt TAŞ

ABSTRACT

DIP-COATING OF CALCIUM HYDROXYAPATITE ON TITANIUM ALLOY (Ti-6Al-4V) AND STAINLESS STEEL (316L) SUBSTRATES

Maviş, Bora

M.Sc., Department of Metallurgical and Materials Engineering

Supervisor: Assoc. Prof. Dr. A. Cüneyt Taş

January 1999, 67 pages

Stainless steel (316L) and the titanium alloy (Ti-6Al-4V) are commonly used biomaterials as load-bearing implants in numerous orthopedic applications, such as the repair and healing of human bones. The main inorganic phase of human bones is calcium hydroxyapatite (HA: $Ca_{10}(PO_4)_6(OH)_2$). When a metallic implant and human bone are brought into contact, a mutual interaction is initiated via surface reactions. To what extent bone-plus-metallic implant will be able to function as an integrated mechanical unit depends on the chemical, physical, and mechanical characteristics of the living bone and the bioinert metallic implant. To achieve the high tensile strength necessary for load-bearing implants, metal alloys, such as 316L or Ti-6Al-4V, can be coated with the bioactive calcium hydroxyapatite bioceramics. Dip-coating of HA onto metal-based high-strength bioimplants is a scarcely experimented technique in biomedical technology. The experimental details of the development of novel suspensions of chemically-precipitated sub-micron HA powders used in the dip-coating of stainless steel (316L) and titanium alloy (Ti-6Al-4V) substrates are hereby presented. Sample characterization is mainly achieved by SEM, EDXS, and XRD.

Keywords : Dip-coating, calcium hydroxyapatite, bioceramic

ÖZ

KALSİYUM HİDROKSİAPATİT'İN DALDIRMA-KAPLAMA YÖNTEMİ İLE TİTANYUM ALAŞIMI (Ti-6Al-4V) VE PASLANMAZ ÇELİK (316L) YÜZEYLERE KAPLANMASI

Maviş, Bora

M.Sc., Metalurji ve Malzeme Mühendisliği Bölümü

Tez Yöneticisi: Doç. Dr. A. Cüneyt Taş

Ocak 1999, 67 sayfa

Paslanmaz çelik (316L) ve titanyum alaşımı (Ti-6Al-4V), pek çok ortopedik uygulamada, insan kemiklerinde oluşan defekt'lerin tedavisinde sıklıkla kullanılan, yük-taşıyabilen biyomalzemelerdir. İnsan kemiklerinin esas inorganik fazı kalsiyum hidroksiapatit (HA: $Ca_{10}(PO_4)_6(OH)_2$)'tir. Metalik bir implant ile insan kemiği birleştirildiğinde, yüzey reaksiyonları ile karşılıklı bir etkileşim başlamaktadır. Kemik-metalik implant ikilisinin entegre olmuş bir birim olarak ne ölçüde davranabileceği, her ikisinin kimyasal, fiziksel ve de mekanik özelliklerine bağlıdır. Yük-taşıyabilen ve yüksek çekme mukavemetine sahip implant'lerin eldesinde, 316L veya Ti-6Al-4V gibi metallerin yüzeyleri, biyoaktif HA biyoseramikleri ile kaplanabilmektedir. HA'in daldırma-kaplama yöntemi ile metal-esaslı, yüksek mukavemetli biyoimplant'lere kaplanması biyomedikal teknolojide oldukça az olarak denenmiştir. Burada, kimyasal yöntemler ile çöktürülmüş, mikron-altı HA tozları kullanılarak özgün daldırma-kaplama suspansiyonları geliştirilmesinin deneysel detayları sunulmuştur. Numune karakterizasyonu SEM, EDXS ve XRD çalışmaları ile gerçekleştirilmiştir.

Anahtar sözcükler: Daldırma-kaplama, kalsiyum hidroksiapatit, biyoseramik

to my Parents and Elif

ACKNOWLEDGMENTS

I express my sincere appreciation to my thesis supervisor Assoc. Prof. Dr. A. Cüneyt Taş for his guidance and close collaboration at every stage of this research.

I also thank to my family and friends for nothing in particular, but everything in general.

I would like to express my sincere appreciation to the Graduate School of Natural and Applied Sciences for providing me a research assistantship throughout the course of this study.

My sincere thanks should also go to Mr. Hakan Ertürk and Mr. Emre Altuğ Yavuz, for their suggestions and helps in transforming an old hammer design into a brand-new dip-coating machine that is used in this study.

TABLE OF CONTENTS

LIST OF TABLES

TABLE

LIST OF FIGURES

FIGURE

CHAPTER 1

INTRODUCTION

Stainless steel (316L) and the titanium alloy, Ti-6Al-4V, are two of the bioinert load-bearing implant materials of high modulus of elasticity values, which are commonly used in clinical orthopedic applications. Insertion of a biomaterial in a living hard tissue, such as bone, creates an artificial interface between living tissue and biomaterial. An ideal interface should behave in the same way as a theoretical plane present at the same place in the healthy tissue. When an implant and tissue are brought into contact, a mutual interaction is initiated via surface reactions. At the interface, primary reactions will take place either on the atomic scale, such as dissolution of ions from the material, or on the molecular scale, such as protein adsorption and desorption.

To what extent bone-plus-implant will be able to function as an integrated mechanical unit depends on: the mechanical and physiological characteristics of the living bone; the chemical, mechanical and physical properties of the implant, and the interaction between bone and implant.

The main inorganic phases of bones and teeth of vertebrates as well as hard tissues of humans appear to be predominantly in a single structural state closely resembling that of calcium hydroxyapatite, $Ca_{10}(PO_4)_6(OH)_2$. Because the mechanical properties of synthetic calcium hydroxyapatite bioceramics are limited, they should be loaded only in compression.

To achieve the high tensile strength necessary for load-bearing implants, metal alloys, such as 316L or Ti-6Al-4V, can be coated with calcium hydroxyapatite particles. The superior bone bonding capacity and the bioactive nature of synthetic calcium hydroxyapatite may help earlier stabilization of the bioceramic-coated metallic implant in the surrounding bone.

Current industrial and laboratory techniques used for coating HA bioceramics onto metallic substrates include plasma spraying, electrophoretic deposition, sputtering and hot isostatic pressing. However, all of these techniques would either yield non-crystalline coating layers or coat layers contaminated with crystalline calcium phosphate phases other than HA.

Dip-coating of HA onto metallic substrates is a scarcely experimented technique in this field of technology, although it is potentially advantageous as compared to others in providing 100% crystalline and phase-pure HA coatings.

In the present study, the experimental details of the development of novel suspensions of chemically-precipitated sub-micron HA powders used in the dip-coating of stainless steel (316L) and titanium alloy (Ti-6Al-4V) substrates are presented.

CHAPTER 2

PREVIOUS WORK

2.1. Synthesis of Calcium Hydroxyapatite Powders

Chemically-precipitated calcium hydroxyapatite (HA: $Ca_{10}(PO_4)_6(OH)_2$) powders have first been prepared by Hayek and Newesely in 1963 [1]. In the typical chemical precipitation routes used for HA synthesis, solutions of calcium nitrate tetrahydrate ($Ca(NO_3)_2.4H_2O$) and di-ammonium hydrogen phosphate ($(NH_4)_2HPO_4$), of proper concentrations, were reacted with one another at high pH-values in the presence of ammonium hydroxide (NH_4OH) [2-7].

HA powders prepared and used in this study have been synthesised by using the previously published and patented method of Taş [8, 9], which was basically a modification of the route of Hayek and Newesely [1]. The powders of this study, were synthesised by chemical precipitation from aqueous solutions of calcium nitrate and di-ammonium hydrogen phosphate salts, and were found to have high phase purity with an average particle size of 0.6 to 0.7 μm and relatively high surface areas in the range of 40 to 45 m^2/g [10].

Improved thermal stability, phase purity, chemical uniformity, and good dispersion behaviour in aqueous or alcoholic solutions and slurries were the desired set of properties from powders to be used in dip-coating studies.

2.2. Coating of Metallic Implants

The main inorganic phase of natural bones appears to resemble HA. However, it contains foreign ions, such as CO_3^{2-}, Mg^{2+} and Na^{+}, and some trace metal ions, like Fe, Zn, Cu, etc. Due to its greater resemblance to the biological HA, synthetic HA could be used as a bone substitute or graft material. The proposed biocompatibility of HA was not only suggested from its composition point of view, but also due to the *in vivo* experiments that have been conducted. New bone ingrowth into synthetic HA prostheses, after implantation, to which the term *osteogenesis, osseointegration,* or simply, *new bone formation* was commonly assigned, has been demonstrated by a number of clinical works [11, 12]. HA implants were always found to be highly biocompatible, in *in vivo* studies, since it did not produce any local and systemic toxicity, inflammation, and foreign body response.

On the other hand, the mechanical properties of the man-made calcium phosphate ceramics were just limited to be sufficient only under compressive loading cases. Use of these materials as tensile load-bearing implants is nearly impossible due to their brittle nature, low fracture toughness, and low resistance to impact loading. Whereas, metals such as titanium and its alloys, and to certain extent, stainless steels and cobalt-chromium alloys, *e.g.*, Ti-6Al-4V, 316L, have sufficient mechanical strength and can easily be machined. The above-stated materials have been widely used in biomedical load-bearing implantation applications, also due to their high corrosion resistance and toughness.

The best use of HA in load-bearing implant applications was considered as a coating layer on one of such strong implant metals. Uncoated metal surfaces are generally responsive to the tissues surrounding them, however, coating of these surfaces prior to implantation by some means, will be conducive in new bone formation, that is it will enhance osseointegration [13-47].

The first trials on the coating practice were performed by using thermal spraying techniques, among which plasma spraying (PST), have taken most of the attention through the recent decades. The PST has now been applicable in the commercial-

scale. However, most of the literature has been concentrated on the methods of overcoming the drawbacks of the technique itself, like water vapour treatments or post-plasma-spray heat treatments. These drawbacks, generally arising from a variety of parameters that have to be controlled during coating, *i.e.*, particle size of the powder used, type and purity of the gas chosen, speed of plasma, distance of the substrate from plasma core, and cooling scheme of the coated surface. Crystalline phases other than HA and amorphous calcium phosphate (ACP) material can be formed in different amounts, due to small changes in the process flow or high temperatures experienced by the ceramic particulate. The high temperatures used in thermal spraying practices also affect the thermal treatment history of the substrates significantly. The low crystallinity of the final coating layer was proven to cause the higher rates of dissolution of the HA coatings upon implantation. To allow full stabilisation in bone, a non-metallic layer of coating should remain intact on the implant for a sufficient time. This should not be confused with the phenomenon called *biodegradation.* The coating phase deposited on prostheses, for such time-dependent *in vivo* processes, may sometimes intentionally contain *bioresorbable* TCP or ACP; in order to adjust the coating dissolution rate nearly equal to that of the new bone formation [13-19].

However, mainly due to the severe difficulties encountered in the achievement of highly crystalline coatings, also with reproducible adhesion strengths, by using the plasma-spray technique, alternative low-temperature techniques have been investigated for the coating of bioceramics on metallic surfaces.

High velocity oxy-fuel technique is the low-temperature version of the PST and solved the problem of low crystallinity of HA to some extent. Near room temperature techniques tried on calcium phosphates provide another list of solutions consisting of electrophoretic deposition (ED), hot isostatic pressing (HIP), ion beam sputtering (IB), radio frequency sputtering (RF), laser ablation, coatings in biomimetic (37°C and pH=7.4) environments (SBF: synthetic body fluid), blast coating (BC) and sol-gel methods.

Electrophoretic deposition (ED) is useful in depositing HA on porous surfaces, which is not quite possible with the plasma-spray technique [20, 21]. High temperature sintering was needed, since the strength of the coatings was low. Contamination risk from the electrolytes was another problem, which can commonly be faced in all ED practices.

Having an amorphous nature upon deposition, the IB- or RF-coated HA bioceramics [22, 23], needed a low-temperature crystallization treatment (such as 500°C), following the coating. These IB or RF methods are essentially thin-film deposition techniques and the resultant HA coatings with thicknesses ≤ 1 μm were found to be doubtful for their long-term durability in the body environment.

The essential requirement for an artificial material to bond to living bone is the formation of a bone-like apatite layer on their surfaces. Many researchers [24-31] have been trying to mimic this well-known phenomenon by *in vitro* experiments. The bone bonding strength of these coatings were significantly altered by the surface conditions of the substrates. To enhance the activity of substrate surface prior to soaking in SBF, either a two-step surface treatment or an additional coating that would deposit an hydrogel over the substrate was found essential.

Kokubo, *et al.* [24-26] have always observed an acicular or needle-like microstructure for the coated HA in their body fluids; however, Taş [27, 28] observed (by working with a slightly different synthetic body fluid) nodular and sphere-like HA particles being nucleated on either Ti-6Al-4V or 316L strips immersed in SBF solutions, at 37°C and pH=7.4, in 1 to 21 days.

Blast coating (BC) of HA by an ordinary sand-blaster seemed [32] to offer a cheap alternative among other room-temperature coating methods. The strength of such coatings was tested by "nail-scratching" and "ultrasonification (for 5 minutes)." These tests were applied to the coatings to see whether the HA coatings would stay intact during the implantation procedure or not. The coatings were reported to successfully pass these tests, and the method was concluded to be superior to other room temperature alternatives, like electrophoretic deposition and dip-coating. The

thickness of the coating, which could only be measured by us from a figure in the manuscript of this study was about 3 μm. The small coating thickness value of this study may pose a question on its long-term durability under *in vivo* conditions.

Barbosa, *et al.* [33, 34] tried to determine the optimum coating thickness that should be achieved to inhibit the metal ion release from the Ti-6Al-4V and stainless steel substrates. 50 μm-thick HA coatings were reported to prevent the release of metal ions into the surrounding physiological medium either by the metal phosphate formation reactions taking place on the coating surfaces or the incorporation of metal ions in the HA structure of the coating.

Long, *et al.* [35] in a review paper on titanium metal noted that if the substrate volume change was a quality-determining factor in an application, then the $\alpha \rightarrow \beta$ allotropic transition temperature of titanium should have been taken into account. Filiaggi, *et al.* [15] considering this fact tried not to exceed 960°C in their heating programs, mainly to prevent stresses that would otherwise arise from such allotropic volume changes.

2.3. Technique of Sol-Gel Dip-Coating

Sol-gel dip-coating (SGDC) consists of the withdrawal of a substrate from a fluid solution associated with gravitational draining and solvent evaporation with a net result of the deposition of a solid film on the substrate surface. Compared with sputtering or chemical vapour deposition, SGDC requires less equipment spenditure, and therefore, it is less expensive. Moreover, it gives the operator a chance of controlling or tailoring the microstructure of the deposited films.

The only requirements for the success of the films are that the condensed phase should remain well-dispersed in the solvent or vehicle, macroscopic gelation be avoided, and that the solution (sol) be dilute enough, so that upon coating the critical crack thickness not be exceeded. These thicknesses were reported [36] to be between 0.5 and 1 μm. One way of avoiding cracks has been the use of plasticizers in the

manufacture of organic polymer films. Analogous results were also obtained in sol-gel systems.

In SGDC, the substrate is generally withdrawn vertically from the coating solution at a constant speed U_0. Figure 2.1.a. (figure adopted from [36]) showing the sequential stages of structural development that result from draining accompanied by solvent evaporation and continued condensation reactions, where U_0 is the withdrawal speed, h(x) is the film thickness at position x measured from the drying line x_0, h_0 is the entrained film thickness just above the stagnation point S, η is the liquid viscosity, ρ is the liquid density, P_C is the capillary pressure, γ_{LV} is the surface tension, and θ is the wetting angle. The moving substrate entrains the liquid in a viscous boundary layer, which then splits it into two at the free surface. Figure 2.1.b. (figure adopted from [36]) gives the detail of flow patterns, where δ is the boundary layer, and h is the thickness of the fluid film. As the film becomes more concentrated in the condensed phase through evaporation, the rheological response of the entrained solution changes until viscoelastic behaviour is reached. Extending gelation over the film force it to behave more or less as an elastic solid. It is at this stage that the capillary pressure P_C created by tiny menisci as they recede into the gel is maximized. The curvature of the menisci causes the liquid to be in tension and the network in compression. The capillary pressure represents a very strong driving force to densify the depositing film. It is the balance between this capillary pressure, which compresses network, and the modulus of the network, which enables it to resist collapse, that establishes the final density and pore size of the film (Fig. 2.1.a.). As the solvent evaporates, the gel is able to shrink.

Upon careful inspection of the general theoretical aspects of the SGDC technique, one comes up with the following observations:

1. Due to the short scale of film deposition process, introduced by SGDC, condensation reactions in the used organic constituents may not have enough time to take place. Therefore, rather than a direct chemical condensation, a physical condensation takes place due to the strong concentration dependence of the viscosity. Immediate resolubilization of the formed-film, if immersed back in the solvent, was taken to be a proof of this fact.

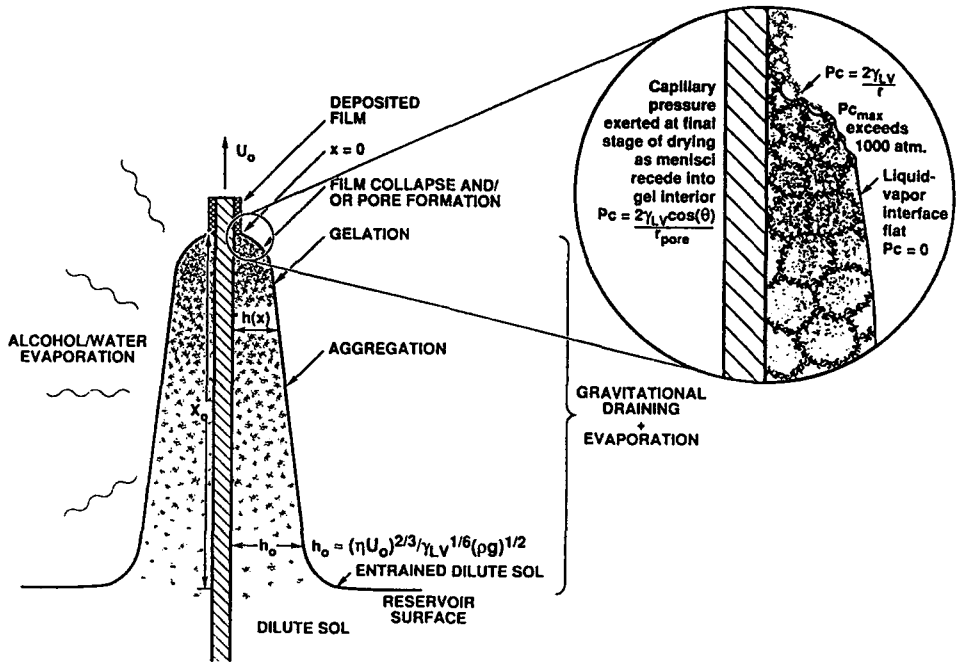

Fig. 2.1.a. Schematic of the steady-state dip-coating process [36].

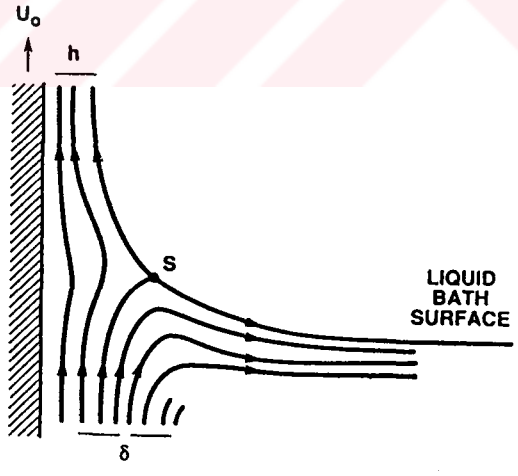

Fig. 2.1.b. Detail of flow patterns (streamlines) during dip-coating [36].

2. Two component solvent mixtures, like the ones used in this study, for instance, that of water and ethyl alcohol, were reported to form two menisci at the solution-substrate interface during the withdrawal. The surface tension gradient forming in these two menisci increases the shear rate of consolidation and improves the alignment of the dispersed inorganic solute.

3. The type and size of organic, its condensation rate, and the time scale of deposition would all influence the final porosity of the coatings.

It is possible to have a control on the structural properties (i.e., pore size and volume, surface area, and refractive index) of the deposited films by inducing controllable changes on size of the solid particles, relative rates of condensation and evaporation, capillary pressure and substrate withdrawal speed. SGDC is a rugged and flexible technique in the sense that any substrate geometry is also acceptable [36].

The SGDC method has been applied to quite a lot of systems containing ceramic oxides, such as indium-tin oxide, ZnO, TiO_2, Nd:YVO_4 and Al_2O_3. The withdrawal speeds applied during the above-mentioned coating studies were varied within the range of 6 to 130 mm/min [37-42].

Haddow, *et al.* [42, 43] studied the SGDC of TiO_2 films on titanium substrates. The high level of biocompatibility of titanium implants in the body environment stems from the *osteoconductive* properties of the naturally (i.e., *in vivo*) formed titania layer covering the implant surface. Haddow, *et al.* tried to coat glass cover slips, which are bioinert, with the TiO_2 by using the SGDC technique. With the typical withdrawal speeds of about 6 mm/min, they reported to obtain 30 nm-thick coatings. These coatings were thicker than the naturally occurring ones on the titanium surfaces. However, they claimed that the coating thickness could further be decreased by diluting the dip-coating solution. They also observed an unpredictable coloration on their coatings (in the titania layer) and suggested that this could be due to the valency change observed in Ti-ion (between the values of 3+ and 4+) during soaking at the peak firing temperature.

2.4. Sol-Gel Dip-Coating of Calcium Hydroxyapatite

Haddow, *et al.* [43] worked also on apatite-like coatings by using the technique of SGDC. They extended the firing temperature up to 1200°C, and used zirconia disks as the bioinert substrate which were prepared by hot pressing. The disks were polished with 1200-grade SiC papers. They coated their substrate with different solutions containing dissolved Ca and P ions, which were prepared according to the stoichiometric ratio of Ca and P found in HA, *i.e.*, Ca/P = 1.67. Withdrawal speeds of up to 150 mm/min were experimented. Only the precursors prepared from the calcium acetate and triethyl phosphate yielded coatings in which the stoichiometric Ca/P ratio of HA could be approached. A grey colour that was observed in the powders prepared at 800°C indicated the presence of the residues of the organic species used in solutions. DTA traces were provided to prove that the organics could only be completely burned out at about 950°C.

It should be remembered at this point that the substrates used in the study of Haddow, *et al.* [43] were not metallic. Metals, if used as substrate materials in HA coating, on the other hand, are susceptible to serious microstructural changes upon heating at high temperatures. The significant volume change observed in titanium and its alloys during its $\alpha \rightarrow \beta$ transition in the temperature range of 880 to 960°C, and the excessive grain growth seen in stainless steels are just two of the problems associated with the use of metallic substrates in SGDC. Excessive coating shrinkage and beading, as compared to that of substrate, during heat treatment would then result in a final coating of non-uniform thickness.

Baptista, *et al.* [44] have recently used an alkoxide route to produce HA and its coatings. Various combinations of Ca glycoxide and alcoholic solutions of P_2O_5 were studied in terms of the suitability of the obtained powders for SGDC. Powder suspensions were stabilised by the presence of acetic acid, whereas a strict control on the amount of it was also needed to ensure the resulting Ca/P ratio in the powders to match with that of stoichiometric HA. Alumina substrates were withdrawn from such solutions at the typical rate of 40 mm/min. The as-withdrawn films were dried at 150°C for about 15 min, and the dried film was then heated at 500°C for 10 min. To

increase the coating thicknesses to the desired levels, they have applied 10 consecutive dip-coatings on each sample. Coatings were finally heated at 750°C and 1000°C for 15 min each. In the X-ray diffraction (XRD) patterns, peaks coming from the alumina substrate were also observed. Adhesion strengths measured on the specimens heated at 1000°C were found to be in the vicinity of 10 MPa. The scanning electron microscope (SEM) observations revealed some signs of agglomeration among the powders, however these aggregates were claimed [44] to be essential for the promotion of new bone formation on such "rough" implant surfaces.

Carsten, *et al.* [45] tried coating of metal substrates with bioactive glass-ceramics. However, the results of the dipping of prothecast and titanium substrates into a "bioverit" melt were inconclusive from the manuscript of this study. Coated layers, with thicknesses ranging between 1 and 2 mm, were observed to possess a lot of cracks and the adhesion strength of those was very low.

Breme, *et al.* [46] aimed to develop a new titanium alloy which has its thermal expansion coefficient shifted more towards that of HA, in order to prevent the tensile stresses to form during cooling from the annealing temperatures. These stresses are known to decrease the adhesion strength of the coatings. In order to test the results of this metallurgical alloying operation, they studied two different ways of coating the substrate. The first approach was the direct sintering of HA powders on the titanium surfaces with and without a bonding agent. Drying of the coatings were achieved at 60°C in 15 min, burning-out (in case of using a bonding agent) was performed at 600°C in 15 min. The HA layer was produced by heating the powders spread on the metal surface at 1200°C.

The second method [46] was a sol-gel procedure, which utilised a mixture of CaO and organic compounds, triethylphosphate and trimethylphosphate in the dipping solutions. Dipping of substrates into the above mixture of starting chemicals was followed by a drying for 1h at 130°C, which resulted in a gel. The coatings were developed after annealing between 600 and 800°C (5 to 15 min). They have also developed a special alloy of Ti, containing 6% Mg. Thin coatings of 1 μm were

produced on such alloys. As stated before, the low thickness of such micron-thick coatings may pose some doubts on the long-term durability of these in the body environment. Peaks of TiO_2 and Ti were observed in the XRD diagrams of those coatings heated at 800°C. On the other hand, SEM micrographs showed the achievement of dense and crack-free coating layers. The adhesion strength of HA coatings was reported to be higher than the tensile strength of the glue applied onto it (to remove the coated layer), which had been taken about 70 N/mm^2. Withdrawal speeds were not reported throughout this study.

Ceramic layers coated over the load-bearing material have to sustain the maximum tensile stress under the bending type of loadings, and therefore, the thicker the coatings become, the higher will be the tensile stresses acting on them. The values of coating thicknesses for minimum tension and the values for preventing the metal ion release (*in vivo*) should be balanced and compromised in reaching an optimum thickness value.

Tuantuan, *et al.*, [47] produced HA crystals by reacting together calcium hydroxide suspensions and phosphoric acid solutions under ultrasonic irradiation. The formed HA crystals were then dispersed in distilled water or physiological salt solutions for the preparation of the dipping solutions. Pure titanium rods were dipped in these solutions once and/or seven times. The dip-coated rods, with coating thicknesses ranging between 10 and 200 μm, were then implanted into femurs of a dog. New bone ingrowth with the HA-coated implant (after two weeks *in vivo*) was observed by SEM studies. Sand-blasted rod surfaces were found to be superior to the smooth untreated surfaces. Although the details of the used technique of bone bonding strength measurements were not given in this manuscript, the pull-out strengths (from the natural bone) of the HA-coated implants were reported as twice those of the uncoated implants. Since the coatings were not heat-treated prior to surgery, their wet strength was taken as zero, and within the *in vivo* implantation period (2 to 4 weeks) they were observed to reach a strength of 2.5 MPa. Therefore, Tuantuan, *et al.* [47] concluded that this method could only be useful for quick bone formation. Neither the HA powders formed in this study nor the HA-coated surfaces have been

presented with data on their respective phase distribution. Withdrawal speeds used in the dip-coating process were also not reported.

The study presented here is mainly focussed on the dip-coating of HA on either Ti-6Al-4V or 316L strips, from fine bioceramic dispersions prepared by using sub-micron, novel HA powders mixed with certain organics in aqueous/alcoholic medium. The recipes of the viscous dipping solutions developed in this study were also novel and unprecedented in the available literature.

CHAPTER 3

EXPERIMENTAL PROCEDURES

3.1. Chemical Synthesis of HA Powders

Calcium hydroxyapatite (HA: $Ca_{10}(PO_4)_6(OH)_2$) powders used in this study have been produced in our laboratory in close resemblance to the previously studied and established powder preparation recipes [8-10, 48-51]. The HA powder preparation recipe that was specifically used in the production of the thin laminates of hydroxyapatite [50] was the starting point for this study, since the solutions used for tape-casting of HA were also found to be appropriate for sol-gel dip-coating (SGDC).

However, the powder preparation method employed in this study has seen some slight modifications (as compared to the above-mentioned previous work of our laboratory), as a result of which the powders became more suitable for the SGDC process.

The optimized HA powder synthesis recipe used in this study can be described as follows: *

A 3 mL aliquot of 0.1 gpl (gram per litre) methyl cellulose (MC: Sigma Inc., USA, Lot No: 73H0365) solution was mixed with 1428 mL of distilled water (DW) in a 2000 mL-capacity beaker. 35.706 g of $Ca(NO_3)_24H_2O$ (Merck, Germany, Lot No:

---

* ***Patent Pending***, TPE, Ankara, January 13, 1999.

A815220) was dissolved in the above solution. Then, 11.082 g of $(NH_4)_2HPO_4$ (Merck, Germany, Lot No: A839106) was dissolved in the above solution. 115 mL of 24 vol% ammonium hydroxide (NH_4OH: Birpa, Turkey) was added at once into the above opaque solution. The solution was then heated and vigorously mixed at 60-70°C for 90 minutes on a stirring hot-plate. (Only in powder batch 6 (B6), a boiling step of 15 minutes was added to the end of the above procedure.)

As was the case with our previous studies [8-10, 48-51], powders produced by the above recipe were consisted of single-phase, sub-micron and spherical hydroxyapatite powders.

The three basic changes (as compared to the previous work of Taş, *et al.*) incorporated into this newly patented HA powder synthesis recipe were;

a) elimination of the final step of 2 h of boiling,
b) reduction in the volume of NH_4OH used to about its one third, and
c) addition of a dilute solution of methyl cellulose (MC) as a "dispersant."

In order to maintain a higher level of reproducibility throughout this study, 5 batches of synthesized powders were first left on the bench in their reaction beakers, overnight, for settling; and after removal of the maximum amount of clear solution that was left over the precipitates, these 5 separate batches of wet precipitates (in their mother liquors) were mixed vigorously at room temperature in a new beaker for 1 h. Then, this beaker was placed into a stagnant air oven at 90°C to rapidly evaporate the solution. The recovered powders, without the tedious steps of filtering and washing with deionized water (DIW), were dried until the state of constant weight measured on a 5½-digit precision analytical balance. Large quantities of dried powders that were left over, after water evaporation, were stored for longer times in Zip-Lock® nylon bags, prior to their use in the consecutive SGDC runs.

3.2. Sintering Behavior of HA Powders of the Present Study

For the determination of the sintering characteristics of the "new" HA precursors of this study, the precipitates formed in accord with the above-stated synthesis recipe were not dried in their mother liquors, but those precipitates were recovered from their respective supernatant solutions by filtering with filter paper (Fig. 3.1). The filtrates were then washed three times with DIW, followed by drying at 90°C. The powders used in the preparation of dip-coating solutions were first ground into a fine powder in an agate mortar with an agate pestle, and later calcined at 600°C for 3 h, followed by an overnight heating at 500°C.

Circular pellets (3 mm-thick, 8 mm diameter) were prepared with the calcined powders by cold uniaxial pressing in hardened steel dies at a pressure of 55 MPa. The pellets were separately heated to (and cooled from) the peak temperatures of 840°, 1050°, and 1200°C (with a soak time of 6 h, in an air atmosphere) at the rate of 2°C/min. The phase purity of the calcined (in the temperature range of 90° to 1200°C) powders of this work was investigated by collecting X-ray data via a powder diffractometer (Rikagu, Inc., D-Max/B, Tokyo, Japan) operated at 40 kV, 20 mA, with a $CuK_{\alpha 1}$ monochromated tube, at a step size of 0.05° 2θ and a count time of 1 second.

3.3. Sol-Gel Dip-Coating (SGDC)

3.3.1. Preparation of HA Dip-Coating Solutions

The idea of preparing solutions appropriate for use in further dip-coating research has first been placed in the previous thesis work performed by Şimşek [49] and Yiğiterhan [50]. Especially, the review and the development of the efforts spent on the formulation of suitable tape-casting slurries of HA bioceramics in the work of Yiğiterhan [50] formed the initial stage of the present study.

At the beginning of the present work, the experiments were started from the point of

Fig. 3.1. Filtering of HA powders by gravitational draining, and desiccators with controlled relative humidity.

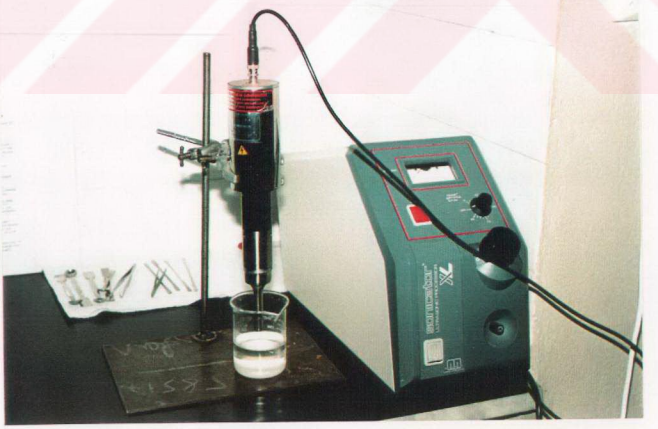

Fig. 3.2. Photograph of ultrasonic disruptor probe (USD)

"reproducing" the best working slurries established in the previous research of tape-casting of HA. For space considerations, much of the work of the initial phase of this study has not been mentioned here.

In the preparation of HA suspensions (in the solvents of ethyl alcohol (EtOH: Aklar Kimya, 96% pure, Turkey) and distilled water (DW) mixtures) useful for SGDC, there had been quite a lot of trials with the use of different organics and with their concentrations in the suspensions. Several organics which were found to act as dispersants, plasticizers, and binders in the tape-casting [50] of HA bioceramics were also experimented with during the studies of the initial stage.

The above-mentioned organics which were tried in this study were as follows; polyethyleneglycol (PEG: Merck, Germany, Mol. Wt.: 15 000, Lot No: A819003), polyethyleneimine (PEI: Sigma Inc., 50 wt% aqueous solution, Lot No: 55H0980), synthetic gelatine (GEL: Riedel-de Haen, Lot No: 42630), glycerol (GLY: Birpa, 99.5% pure, Lot No: 900039), fish oil (FO: Seven Seas, Lot No: 262033), and methyl cellulose (MC). The presence of organics in SGDC solutions generally act to yield a homogeneous dispersion, a final coating with a homogeneous thickness, improved handling in the green (i.e., unfired) state, a higher green body strength due to the elastic gels they form during the dip-coating process, an improved resistance to cracking upon drying, and finally controlled porosity after the burn-out.

The SGDC solutions were mixed under vigorous ultrasonic irradiation by using an ultrasonic disruptor probe (Misonix, Inc., Model XLS-2015, USA), specifically designed to disperse particulated material in solutions, which was photographed in Figure 3.2. The maximum output power that can be driven from the probe tip was rated at 475 Watts. The ultrasonic irradiation levels were scaled as given in Table 3.1. The surface area of the probe was measured to be 1.29 cm^2. The intensity of the ultrasonic energy applied at a specific level was then approximated by dividing the power driven at that level to the probe area. Throughout the text, the use of ultrasonic disruptor probe at a certain irradiation level was abbreviated as USD1 through USD10.

Table 3.1. USD levels, corresponding wattage and intensities driven at those levels.

Irradiation Level	*1*	*2*	*3*	*4*	*5*	*6*	*7*	*8*	*9*	*10*
% Output Power	10	16	18	20	22	26	28	30	32	34
Power Driven (Watts)	48	76	86	95	105	124	133	143	152	162
Intensity (Watts/cm^2)	37	59	66	74	81	96	103	111	118	126

The solution formulation and preparation studies were carried out under the light of important processing parameters of SGDC, such as the effect of fast drying of dip-coated samples on crack formation, the effect of the use of different EtOH concentrations in the solvents on drying rates, the effect of different organic additions on the homogeneity of the coatings.

3.3.2. Preparation of SGDC Substrates

The coatings were performed on either 316L stainless steel or Ti-6Al-4V strips used as substrates. The strips had the typical dimensions of 20 x 7 x 1 (large ones) or 10 x 4 x 1 mm (small ones). The effects of possible surface contamination and the presence of oxide layers were studied either by first grinding the metal strips with 400- to 1200-grade SiC papers, followed by careful washing in distilled water under ultrasonic irradiation, or by dip-coating the strips in their as-is forms. Within this context, we have also studied the effect of grinding scratch directions (i.e., either parallel or perpendicular to the direction of dipping / withdrawal) on the homogeneity and quality of coatings.

Several experiments were also performed on evaluating the feasibility or applicability of the technique of *in situ* (at 37°C and pH=7.4 in biomimetic SBF (synthetic body fluid) solutions) HA coating on such substrates [49]. The details of such coating practices were given elsewhere [49]. The purpose of these experiments

was to test the influence of the presence of a chemically adhered calcium phosphate-based pre-coating layer, prior to the rather physical coating to be provided by SGDC.

3.3.3. Experimental Set-up for SGDC Runs

A belt-and-pulley-type apparatus was designed and built for this study. It has a two-way electronic switch to descend and ascend the substrates into (and out) the dipping solutions, at constant, pre-selected rates. The apparatus was shown in the photographs given in Figures 3.3 and 3.4. The basic advantage of using such an apparatus was the fact that withdrawal speeds (WS) in the range of 15 to 300 mm/min could easily be reached without any undesired vibrations in the specimen holder (Fig. 3.4). WS was measured by descending and ascending a pen across a piece of paper just placed opposite to the moving holder. The pen, by this way, drew a line, giving the distance travelled over a fixed time. Specimen weight was isolated from the important process parameters by the use of a reductive (high torque) electrical motor in driving the belts and pulleys.

3.4. Heat Treatment of Dip-Coated Specimens

Dip-coated specimens were first dried overnight at 90°C in a stagnant air, microprocessor-controlled oven. Calcination of the dip-coated, green HA layers were either performed at the maximum temperature of 840 ± 5°C, in a PID-controlled horizontal tube (mullite) furnace (Protherm, Alser, Ankara, Turkey) under flowing inert atmospheres, or performed in a muffle furnace operated in an air atmosphere in the temperature range of 900° to 1050°C (1 h of peak soaking time), by using heating and cooling rates of 2°C/min.

The heat-treatment schemes used for the dip-coated metal substrates in an inert atmosphere was as follows; initial heating of samples from RT to 500°C (organics burn-out step) at the rate of 2°C/min, then a soak of 15 min at this temperature, followed by another ramp to 840 ± 5 °C at the same rate, for peak soak

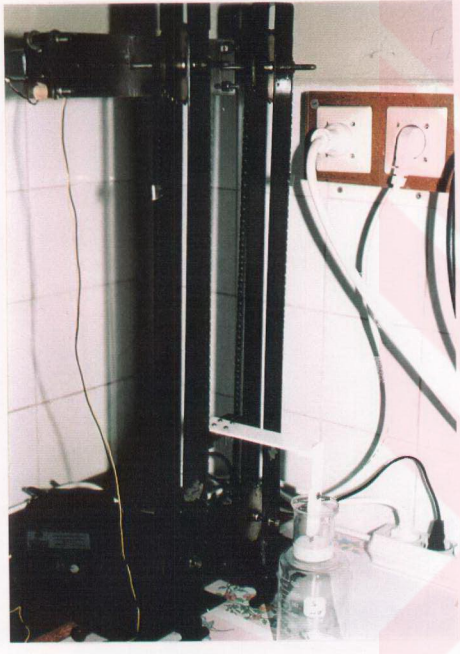

Fig. 3.3. SGDC apparatus designed for this study.

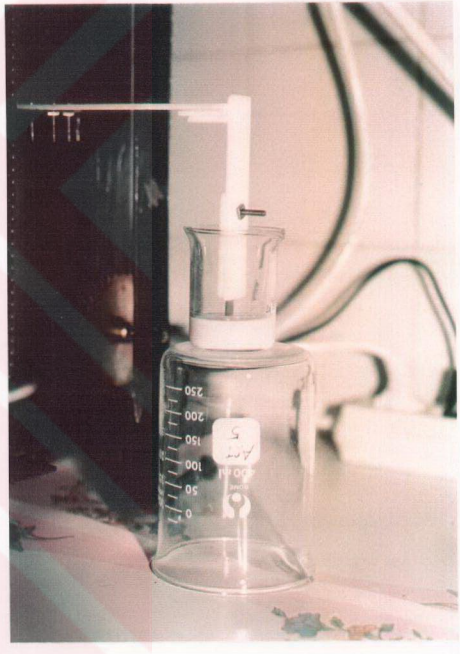

Fig. 3.4. SGDC apparatus designed for this study, specimen holder.

time of 4 h. The samples were then cooled back to RT at the rate of 2°C/min under continuous N_2 flow. The furnace had the necessary attachments to allow its operation under a constant flow (4 L/min) of technical-purity N_2 gas, as shown in Figure 3.5.

Fig. 3.5. Horizontal tube furnace used in the heat-treatment of coatings.

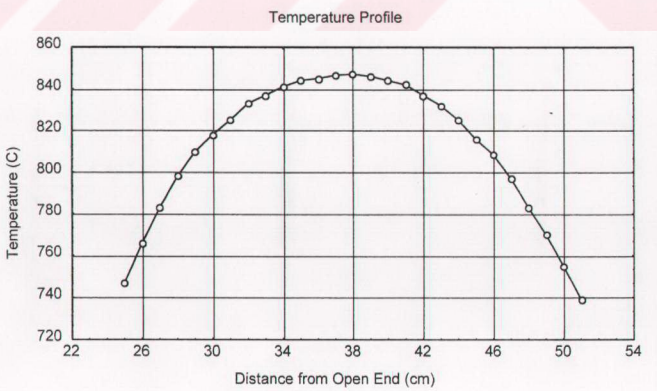

Fig. 3. 6. Temperature profile of the tube furnace (Set T = 850°C).

The exact location of the hot-zone of the furnace was determined by inserting a Type-B (Pt-30%Rh / Pt-6%Rh) thermocouple into the furnace. The temperature distribution in the furnace was obtained from the output of this thermocouple attached to a multimeter (HP, Model: HP34401A, USA). The temperature profile of the heat-treatment furnace was given in Figure 3.6.

3.5. Characterization of HA Coatings

3.5.1. Phase and Microstructure Studies

The coatings applied on glass slides were investigated for the presence of microcracks or coating homogeneity by using an optical microscope (Nikon, Model: ALPHAPHOT-2, Japan). Heat-treated HA coatings were mainly characterized by scanning electron microscopy (SEM: JEOL, Model: 6400, Tokyo, Japan) X-ray diffraction (XRD), and energy-dispersive X-ray spectroscopy (EDXS: Kevex, USA). The EDXS results were believed to be accurate to ± 4%.

3.5.2. Thickness and Strength of HA Coatings

Thickness measurements of the coatings were only roughly performed via SEM micrographs, after tilting the surfaces of the coated metal strips

Ishikawa, *et al.* [32] presented a simple "finger nail scratching" approach in measuring the coating strength, and it was adopted in this study. Dip-coated and heat-treated samples were scratched with the tip of a screwdriver in this study. It should be remembered here that the HA-coated metallic prostheses would only be needed to resist such low-force scratches during handling and implantation by the orthopedic surgeon. It is known [32] that the rather fast osseointegration rates would deposit a layer of new bone in a short time, if the prostheses could only be placed in the body without any significant coating deterioration.

CHAPTER 4

RESULTS AND DISCUSSION

4.1. Chemical Synthesis of HA Powders

Synthesis of HA powders by chemical precipitation has previously been achieved [9, 27] and practiced under numerous chemical variations in the work of the present research group. The initial addition of a small concentration of methyl cellulose (MC) to the precipitation solutions was a "*new step*" added into the chemical synthesis route of HA powders from aqueous solutions mainly to achieve "polymeric stabilization" in the dip-coating suspensions.

A polymer molecule, such as the case was with MC, is a molecule of relatively high molecular weight with repeating units or similar units linked by covalent bonds. Polymeric stabilization [52] by the addition of MC into the HA-precipitation solutions was achieved by the mechanism of "steric stabilization," where the macromolecules were attached to the surfaces of HA particles. This was actually a mechanism which prevents the coagulation of newly nucleated HA particles while they were in the mother liquor.

The presence of the molecules of methyl cellulose were expected to perform two things in the HA-precipitation solutions: 1) to display a strong anchoring to the particle surface (by interacting with the hydroxyl groups of the powder particle surface), and 2) to have a sufficient extension of the adsorbed long-chain into solutions to prevent the particles to approach more than few nanometers from one another.

The "new" HA powders synthesized in this study (with the use of a small amount of MC during their synthesis as described in Chapter 3) displayed superior suspension stability in aqueous dip-coating solutions. Solutions prepared for dip-coating resisted sedimentation in a time of even several days, or in some cases, of several weeks. This has been regarded as a positive sign of the presence of "non-coagulated" and "monodispersed" sub-micron HA precipitates in the dip-coating solutions.

The phase purity of these powders was investigated by powder X-ray diffraction and EDXS. The XRD patterns of the powders that were heated at 90°, 600°, 840°, 1050°, and 1200°C are given in Figure 4.1. It was apparent from this figure that the as-precipitated powders (following drying at 90°C) were poor in crystallinity, however, further heating at higher temperatures, in an air atmosphere for 6 hours, improved the crystallinity of the HA powders. These powders were not contaminated by any other phases of the calcium phosphate family of compounds, and they were single-phase calcium hydroxyapatite.

The results of EDXS analysis performed on a pellet of these powders heated at 840°C was shown in Figure 4.2. The intensity analysis from the respective Ca and P lines in this plot indicated that the produced sample is pure calcium hydroxyapatite.

The SEM micrographs given in Figures 4.3.a and 4.3.b show the microstructure of the surfaces of HA pellets (prepared as described in Section 3.2) heated at 1050° and 1200°C, respectively. It has previously been observed [48, 50, 51] that in HA powders synthesized by chemical precipitation in aqueous media, the sintering temperature was in the vicinity of 1200°C. This fact has been confirmed one more time in the present study, and the samples heated at 1200°C showed almost complete densification. The grain sizes in the samples (Fig. 4.3.b) heated at 1200°C for 6 h was in the range of 1 to 2 μm. On the other hand, the samples heated at 1050°C still showed (Fig. 4.3.a) the presence of individual (although agglomerated to some extent due to the advance of necking and bonding) sub-micron (with an average particle size of about 0.25 μm) particles of HA.

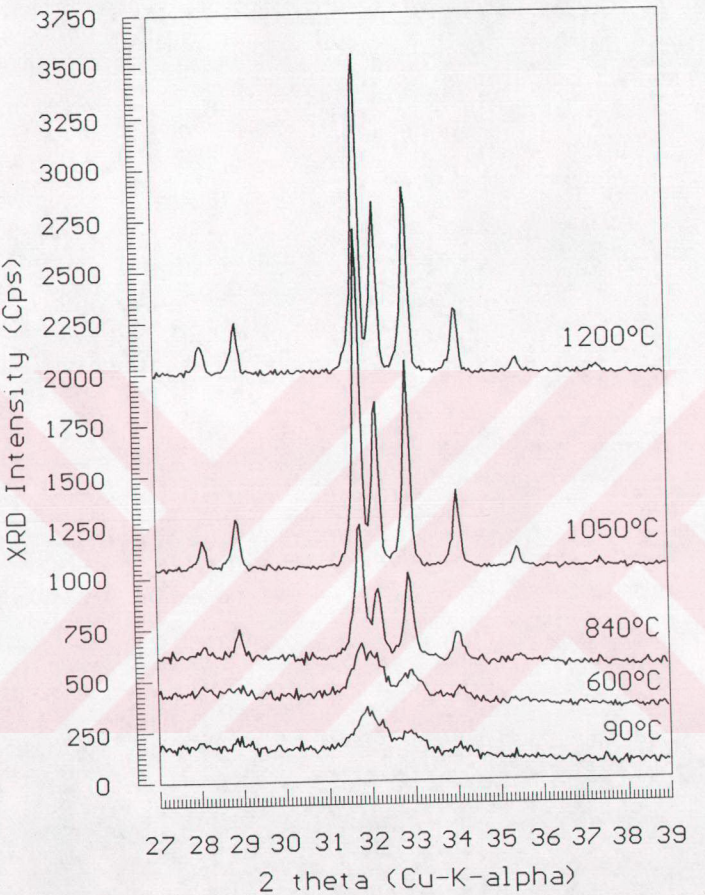

Fig. 4.1. XRD plots of HA powders heated at 90° to 1200°C.

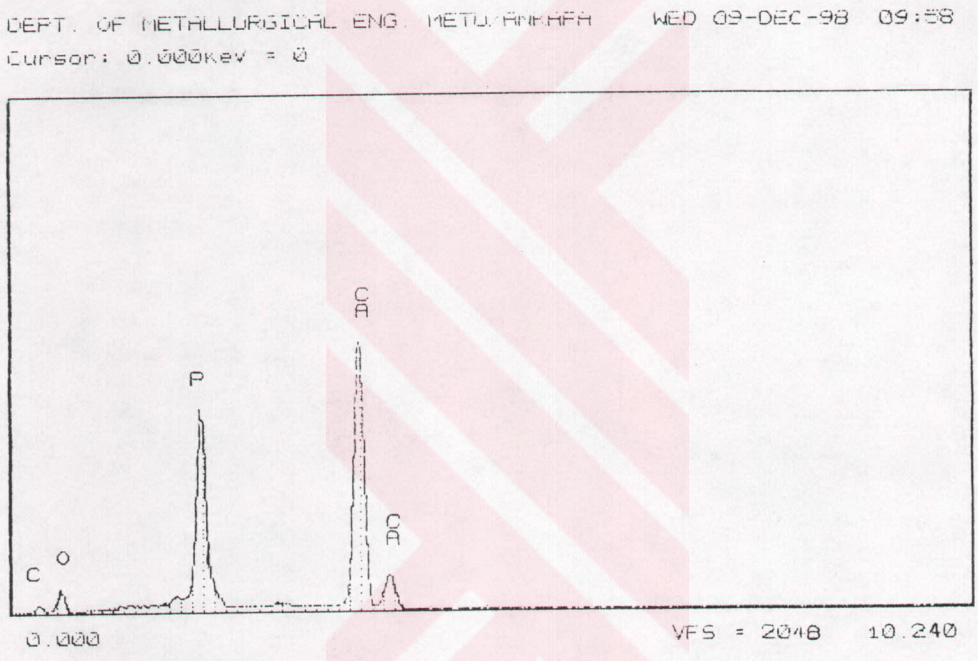

Fig. 4.2. EDXS plot of a HA pellet heated at 840°C.

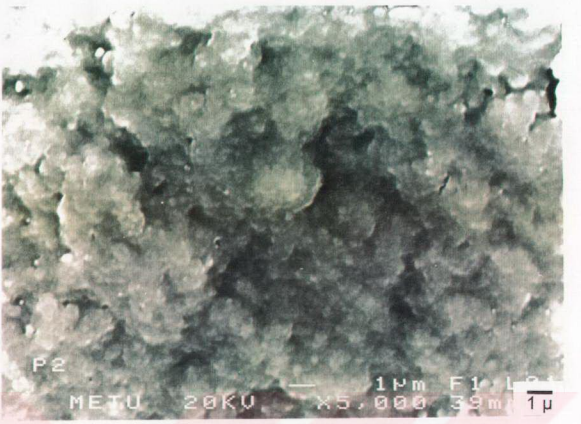

Fig. 4.3.a. SEM micrograph of HA pellets heated at 1050°C.

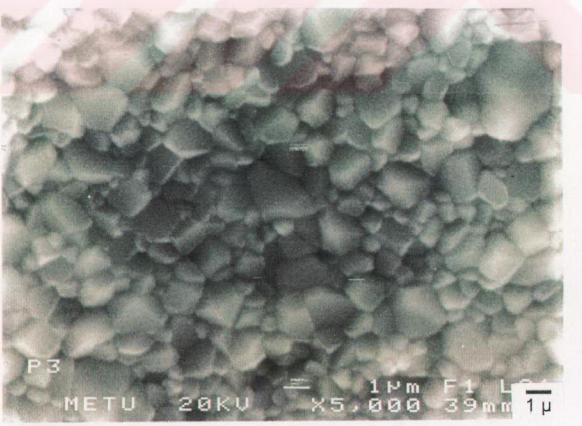

Fig. 4.3.b. SEM micrograph of HA pellets heated at 1200°C.

4.2. Dip-Coating of Calcium Hydroxyapatite Powders

4.2.1. Investigation of the Fundamentals of HA Dip-Coating

The HA powders [9] synthesized without any methyl cellulose additions (during their chemical precipitation) were tested first in terms of their suitability for the dip-coating process. These powders were prepared by using the synthesis procedure as described in Refs. 9 and 50. The dip-coating solutions were then prepared in the following manner; 0.5 g of methyl cellulose, 5 mL of glycerol, 0.75 g of gelatin, and 4 g of HA [50] were mixed in 30 mL of distilled water. The appearance (via SEM micrographs) of these HA coatings, which were performed manually on 316L strips were given in Figure 4.4.a and 4.4.b. The low magnification picture (i.e., Fig. 4.4.a) showed the presence of severe cracks throughout the coating layer. However, these samples were calcined in an air atmosphere at 900°C in a muffle furnace. The uncoated surface of the strips showed extensive formation of an oxide layer. The high magnification picture (Fig. 4.4.b) taken from the coating itself showed that the HA powders had passed through the initial stage of sintering that the necking and bonding of individual particles proceeded. Although the porous nature of the coatings were promising, the presence of cracks and the low adherence of the coating layer due to the presence of severe oxidation problems for the base metal in that case, this sample forms an example for an "unsuccessful" dip-coating trial.

We have also found out during our first trials on dip-coating of HA powders that the dipping operation, when made manually, without using a good working dip-coating apparatus, will only end up with a rough and diffuse solution-coating interface, as shown in Figures 4.5.a. and 4.5.b. These samples were prepared with the same solution described above. This reminded us the strong need for designing and making of a special dip-coating apparatus.

The problem of the oxidation of the base metal (for instance, 316L) when heated in an air atmosphere at 900°C in a muffle furnace was easily solved by using a flowing N_2 atmosphere in a horizontal tube furnace as shown in Figure 3.5. The micrograph shown in Fig. 4.6 belonged to the same dip-coating solution as above, and it showed

Fig. 4.4.a. SEM micrograph showing "unsuccessful" dip-coating trial on 316L.

Fig. 4.4.b. SEM micrograph showing "unsuccessful" dip-coating trial on 316L.

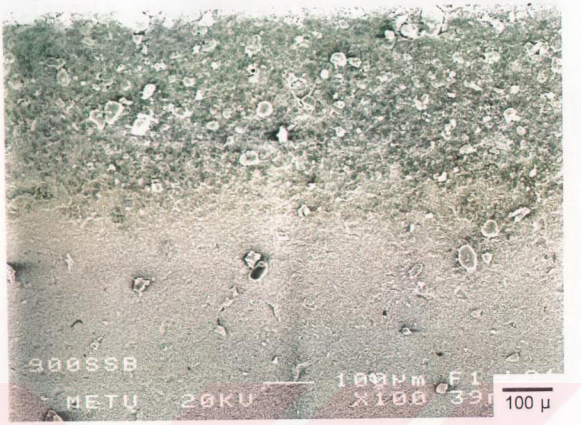

Fig. 4.5.a. SEM micrograph showing "unsuccessful" dip-coating trial on 316L.

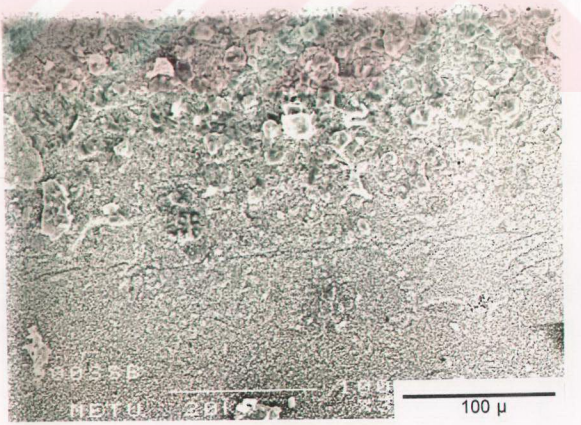

Fig. 4.5.b. SEM micrograph showing "unsuccessful" dip-coating trial on 316L.

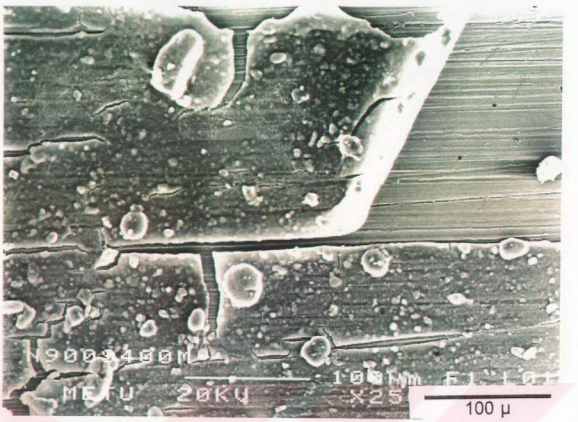

Fig. 4.6. SEM micrograph showing "unsuccessful" dip-coating trial on 316L.

that the intentionally uncoated base metal surface of 316L was free of an oxide layer, and the grinding scratches were even visible after heating it to 900°C. Due to the use of an unoptimized dip-coating solution and HA powder during coating, the coated regions showed the formation of extensive cracks after heat treatment.

Therefore, we have seen that the starting powder used in dip-coating must be free of agglomerates and must have monodispersed particles in it. To this effect, small amounts of methyl cellulose were added to the precipitation solutions as a dispersant. It has also been recognized after the completion of this initial stage of experiments, the formulation of the dip-coating solution to be used has a very strong effect on the final quality of the coating following the calcination step. The presence of macrocracks on the heat-treated sample strongly depended on both the powder quality and the solution recipe employed. On the other hand, the effect of heat-treating atmosphere used (i.e., oxidizing or inert) was shown to have a strong effect on the overall adhesion of coating to the metal. Both the dipping and withdrawal speeds, and the manner in which dipping or withdrawal was performed were also

shown to affect the morphology of the interface to be formed between the base metal and coating.

4.2.2. Preliminary Studies on Solution Search for HA Dip-Coating

The very first efforts towards the determination of "working" dip-coating solution recipes and compositions were performed by the easier or faster technique of dripping few drops of a prepared solution on clean glass slides, and its consecutive examination under a biological optical microscope for the possible presence of cracks (after drying at 90°C). We have decided, at the start of this research, to develop such a solution which ensures "the formation of crack-free coatings without a need for controlled humidity drying." A dip-coating process utilizing such a solution was expected to have important economical advantages in terms of its reduced initial equipment investments by the elimination of expensive slow drying facilities.

It was first observed during the course of this phase of the present study that the bioceramic suspensions prepared by mixing HA powders in distilled water alone, under ultrasonic irradiation, was not successful at all in producing crack-free thick films on glass slides. The pictures taken by an optical microscope given in Figures 4.7.a and 4.7.b displayed the extensive cracking in such films upon drying. The micrograph of Figure 4.7.a belonged to a sample prepared by fine mixing of 1.5 g of HA powders in 25 mL of distilled water (DW). It was always so conclusive that simple mixtures of HA in water would every time display such extensive cracking upon drying.

In a similar fashion, it was discovered that a suspension prepared as-above by adding 0.4 g of gelatin (GEL) into a mixture of 1.5 g of HA powder and 25 mL of distilled water again yielded a deposit with extensive cracking (Fig. 4.7.b).

In the case of using pure water as the solvent in the simple technique of dripping solution drops onto glass slides, as compared to the use of a higher volatility solvent,

Fig. 4.7.a. Micrograph of the film produced from a mixture of HA and DW.

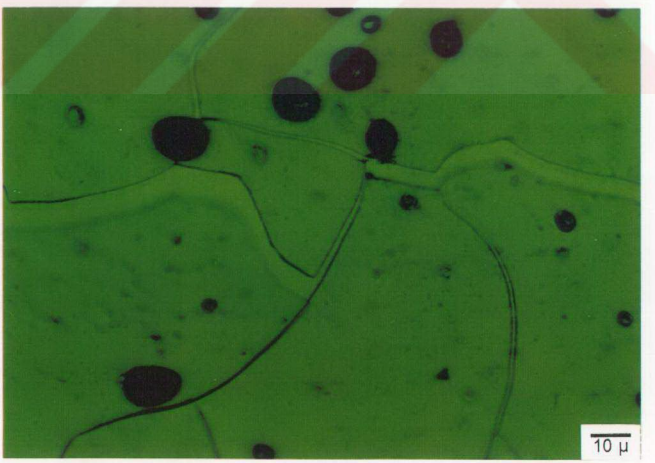

Fig. 4.7.b. Micrograph of the film produced from a mixture of GEL, HA & DW.

such as ethanol, slower evaporation rate and higher surface tension of water cause the wet suspension to flow to the center of the drop before the evaporation of the solvent is completed. The higher magnitudes of capillary pressures attained in this process then causes the formation of cracks.

It is known that [36] during dip-coating, as a consequence of the rather rapid evaporation of the selected solvent and gravitational draining, the inorganic powder particles starts to aggregate, then pass into the stage of gelation (see Fig. 2.1.a). This causes the observation of a "drying-line" having a well-defined geometry, determined mainly by the capillary forces acting. Upon the equalization of the rate of formation of this drying-line with the withdrawal speed of the substrate, one reaches the conditions of steady-state. This essentially ensures the formation of a successful, crack-free coating on the substrate.

For this reason, we have selected to use binary ethanol-water mixtures in the development of solution recipes for our dip-coating experiments. In such mixtures, the differences in the evaporation rates and surface tensions of individual components alter the film profile (Fig. 2.1.a). Preferential evaporation of ethanol then leaves behind a water-rich fluid in the film profile. This phenomenon is called as "Marangoni effect" [36, 53]. This surface tension gradient-driven flow of liquid can create high shear rates during dip-coating. Such shear forces could be sufficiently strong to align or order the entrained inorganic species.

4.2.3. Intermediate Guidelines in the Search of a Working Dip-Coating Recipe

At this stage of this study, it has been recognized that a successful recipe in the preparation of "working" HA dip-coating solutions should have the proper combinations of either gelatine, glycerol or polyethylene glycol in a solvent mixture of EtOH and water.

It has also been considered at the present phase of this study that the surfaces of the metal strips might contain some degree of surface roughness (to improve the adherence of the coated layer of HA after calcination) which could be achieved either by grinding, or even in the form of the presence of a pre-coating with HA particles [27, 49]. Figures 4.8.a and 4.8.b show the microstructures of stainless steel strips soaked in synthetic body fluid (SBF) solutions at 37°C and pH=7.4, for 1 and 21 days, respectively. To obtain a certain degree of surface roughness in our strips to be dip-coated, some of the steel samples (when necessary) of this study have been soaked in SBF solutions for only 8 days.

It has again been realized at this phase of this study that the use of a well-designed automatic dipping (and withdrawal) apparatus should be regarded as necessary to obtain smooth coatings.

The necessity of the use of an inert atmosphere (which could easily be achieved by flowing N_2 through the calcination furnace) has also been recognized at the present phase [54] of this work.

4.2.4. Dip-Coating of HA on Stainless Steel (316L) Strips

The surface oxidation behavior of stainless steel strips was first studied. The SEM micrograph given in Figure 4.9.a show the as-ground (1200 grid SiC paper) surface of a typical 316L strip, without any heat-treatment. The same strip of 316L has the microstructure shown in Figure 4.9.b, after being heated at 840°C under a constant flow of N_2, and it exhibits a minimal level of oxidation. However, when a similar strip was heated at 840°C in a stagnant air atmosphere the surface has been oxidized (Figs. 4.9.c (*low mag.*) and 4.9.d (*high mag.*)).

The stainless steel samples to be discussed in this section have been coded as **SS1** through **SS5**, and the corresponding solutions for those were coded as **SOL1** through **SOL4**.

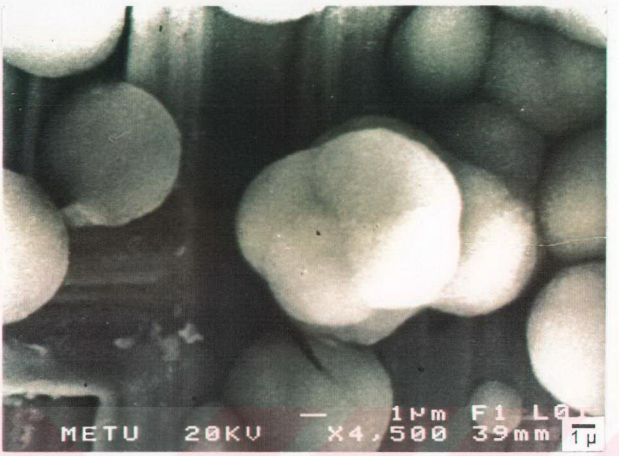

Fig. 4.8.a. SEM micrograph of 316L strips soaked in SBF solutions for 1 day.

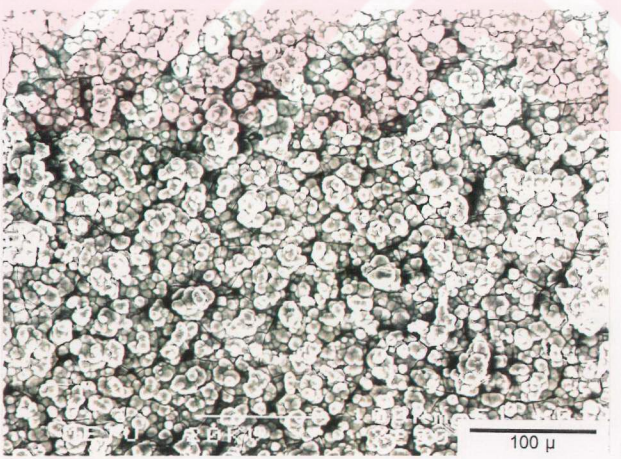

Fig. 4.8.b. SEM micrograph of 316L strips soaked in SBF solutions for 21 days.

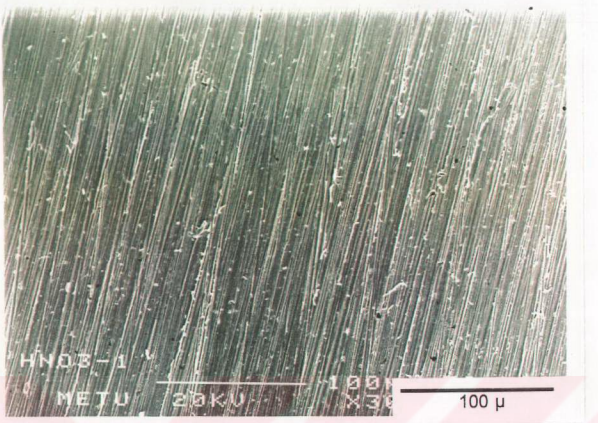

Fig. 4.9.a. SEM micrograph of the as-ground surface of a 316L strip.

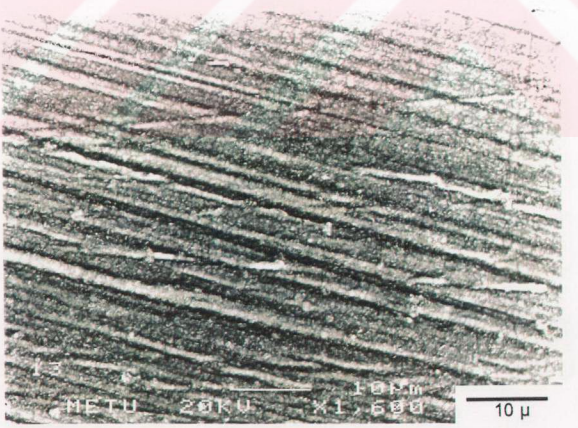

Fig. 4.9.b. SEM micrograph of abraded 316L, after being heated at 840°C under a constant flow of N_2.

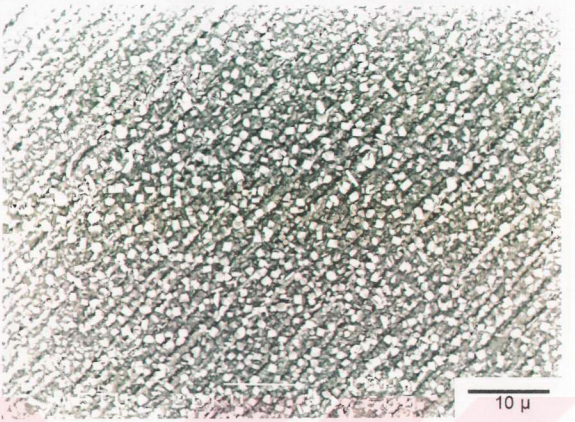

Fig. 4.9.c. SEM micrograph of 316L after heating at 840°C in an air atmosphere.

Fig. 4.9.d. SEM micrograph of 316L after heating at 840°C in an air atmosphere.

The **SS1** samples were first ground with a 400-grid SiC paper in a direction perpendicular to that of dipping, and then pre-coated with a layer of HA particles by soaking in SBF solutions for 8 days at 37°C. The preparation conditions and the formula of the dip-coating solution used in this series of samples were depicted as **SOL1** in Table 4.1. The columns of this table show the material additions to the suspensions. The second or third or fourth columns in the column of a specific material indicate its multiple additions. The **SS1** samples were heat-treated in a flowing N_2 atmosphere at 840°C in a horizontal tube furnace. The coating layers of such samples were investigated by SEM studies. The micrograph given in Figure 4.10.a showed the coat layer-base metal interface in greater detail. Due to the manual dipping of the substrate into the prepared solution, this interface had a quite rough and diffuse nature. The micrograph of Figure 4.10.b, on the other hand, showed the high magnification view of the coating layer. The presence of cracks has basically been ascribed to the fast drying of the green sample at 90°C. This also proved that the solution used for the preparation of these samples was not suitable to resist the fast drying step. The presence of a pre-coated HA layer (coming from the SBF treatment) in the form of bright HA nodules, on the substrate prior to dip-coating, as was seen in Figure 4.10.b, might be a cause of some of those cracks.

The **SS2** samples were first ground with a 400-grid SiC paper in a direction perpendicular to that of dipping, and then pre-coated with a layer of HA particles by soaking in SBF solutions for 8 days at 37°C. The preparation conditions and the formula of the dip-coating solution used in this series of samples were depicted as **SOL2** in Table 4.1. The **SS2** samples were heat-treated in a flowing N_2 atmosphere at 840°C in a horizontal tube furnace. The coating layers of such samples were investigated by SEM studies. The micrograph given in Figure 4.11.a showed the coat layer-base metal interface in greater detail. Due to the manual dipping of the substrate into the prepared solution, this interface had again a quite rough and diffuse nature. However, the dip-coating solutions used for the preparation of the **SS2** samples contained gelatine and a lowered amount of HA powders, as compared to **SS1** samples. The presence of these solution differences, at the first look, suggested that this has been a strong improvement in the final coating quality, exemplified by the observation of less severe cracks (Fig. 4.11.b) across the coat layer.

Table 4.1. Recipe of HA dip-coating solutions*

* ***Patent Pending***, TPE, Ankara

SAMPLE	SOL	HA (g)		H_2O (mL)		EtOH (mL)				PEG (g)			GEL (g)		GLY (mL)
SS1	1	1.517		2		18				0.414	0.257				
SS2	2	1.427	1.131	5	5	20	5	5		0.206	0.200		0.20		
SS3	3	1.427	1.131	5	5	20	5	5	5	0.206	0.200	0.166	0.20	0.06	
SS4	2	1.427	1.131	5	5	20	5	5		0.206	0.200		0.20		
SS5	4	1.311		3		15				0.498					1
TA1	4	1.311		3		15				0.498					1
TA2	5	1.308		2.5		15				0.401			0.06		1.5

SOL	HA wt%	H_2O wt%	EtOH wt%	PEG wt%	GEL wt%	GLY wt%
2	6.90	27.0	64.50	1.10	0.50	-
4	7.30	16.7	66.50	2.80	-	6.7
5	7.24	13.8	66.24	2.22	0.33	10.2

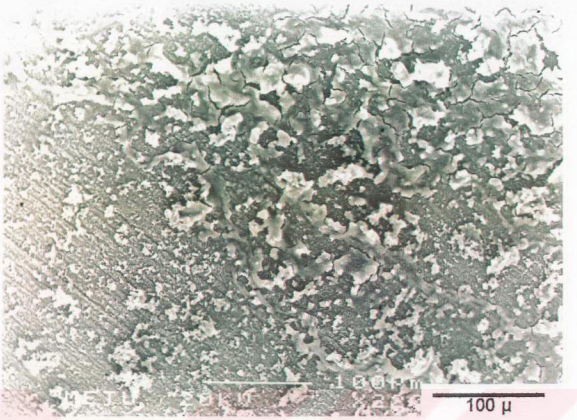

Fig. 4.10.a. SEM micrograph of sample **SS1**.

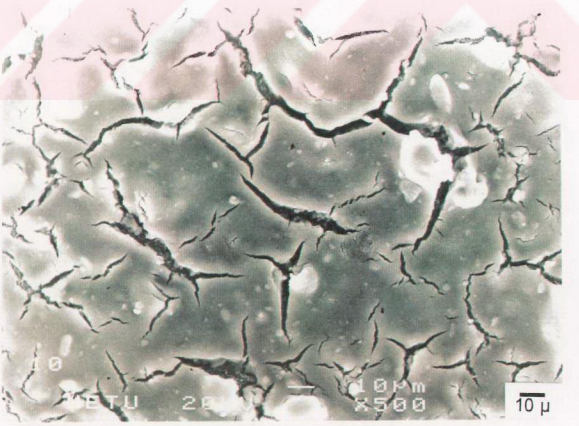

Fig. 4.10.b. SEM micrograph of sample **SS1**.

Fig. 4.11.a. SEM micrograph of sample **SS2**.

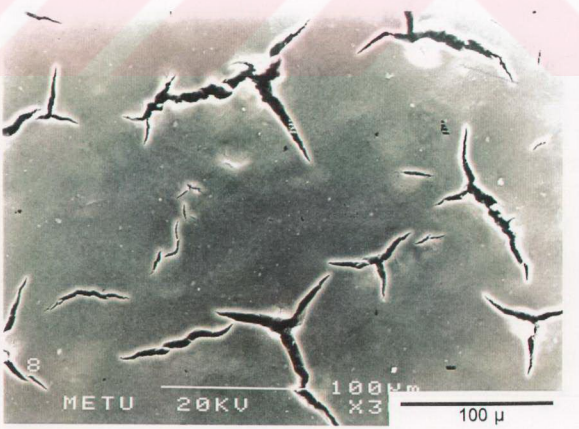

Fig. 4.11.b. SEM micrograph of sample **SS2**.

The **SS3A** samples were first ground with a **400**-grid SiC paper in a direction perpendicular to that of dipping, and then pre-coated with a layer of HA particles by soaking in SBF solutions for 8 days at 37°C. The preparation conditions and the formula of the dip-coating solution used in this series of samples were depicted as **SOL3** in Table 4.1. The **SS3A** samples were heat-treated in a flowing N_2 atmosphere at 840°C in a horizontal tube furnace. The coating layers of such samples were investigated by SEM studies. The micrograph given in Figure 4.12.a showed the decreased concentration of cracks, but it was still apparent that they were basically originated in the vicinity of protrusions created by the nodules of HA coming from the SBF treatment. The **SS3B** samples, on the other hand, were first ground with a **800**-grid (as the only difference from the preparation routine of **SS3A** samples) SiC paper in a direction perpendicular to that of dipping, and then pre-coated with a layer of HA particles by soaking in SBF solutions for 8 days at 37°C. The preparation conditions and the formula of the dip-coating solution used in this series of samples were depicted as **SOL3** in Table 4.1. The micrograph given in Figure 4.12.b showed the overall look of the coat layer taken at a relatively low magnification. It was interesting to note here that as the surface roughness of the initial base metal (or substrate) decreasing (by a passage from 400 grid to 800 grid SiC paper), the surface quality, in terms of the concentration of extensive cracks, of the coating has been slightly improved.

At this point of this research it has strongly been realized that the presence of any protrusions underneath the coat layer was the main cause of crack initiation. This fact was detected to be the case in the micrograph of Figure 4.12.b. The micrographs given in Figures 4.12.c and 4.12.d showed the high magnification views of the nature of coat layers; just on top of a specific protrusion, and within the bulk of a crack-free region, respectively. Therefore, the application of a HA pre-coat layer (via SBF solutions) was actually found to be harmful to the overall quality of the coatings which caused cracks to appear at or near the protrusions of the pre-coat layer. SBF-coating of the substrates was then abandoned throughout the rest of our studies.

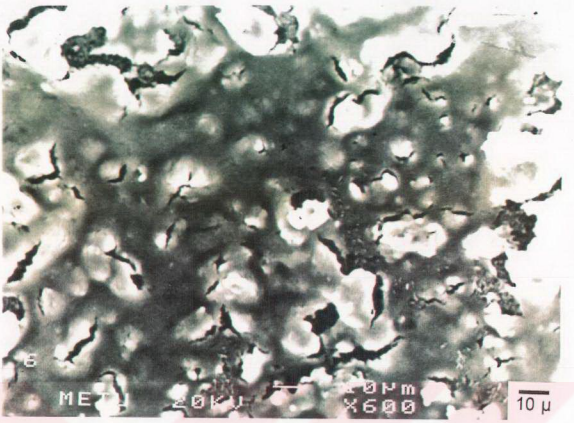

Fig. 4.12.a. SEM micrograph of sample **SS3A**.

Fig. 4.12.b. SEM micrograph of sample **SS3B**.

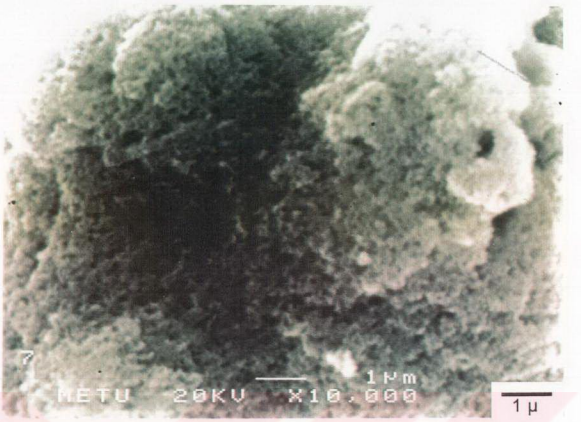

Fig. 4.12.c. SEM micrograph of sample **SS3B**.

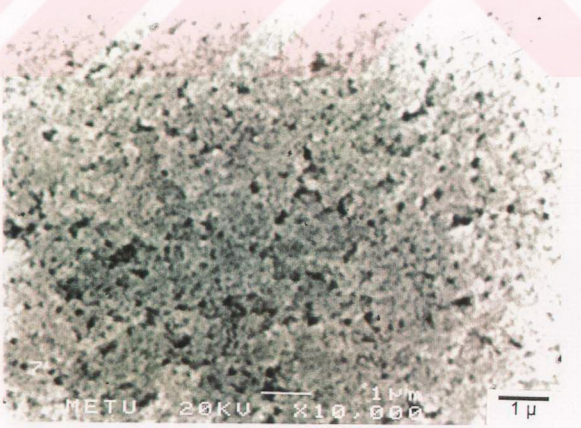

Fig. 4.12.d. SEM micrograph of sample **SS3B**.

The solutions used in the preparation of **SS3A** and **SS3B** series of samples contained slightly increased amounts of the organic additives, i.e., gelatine and polyethylene glycol. The obtained solution recipe, at this point, was found to be satisfactory only when the microstructures of the crack-free regions of the coat layers were considered.

The **SS4** samples were ground with a 800-grid SiC paper in a direction perpendicular to that of dipping which was performed manually. The preparation conditions and the formula of the dip-coating solution used in this series of samples were depicted as **SOL2** in Table 4.1. The **SS4** samples were heat-treated in a flowing N_2 atmosphere at 840°C in a horizontal tube furnace. The coating layers of such samples were investigated by SEM studies. The micrograph given in Figure 4.13.a showed the low magnification view of the coat layer. It was quite interesting to note here that upon removal of the "SBF / HA / pre-coat" step from the overall processing, however, by using the same solution used in the preparation of **SS2** samples, crack-free samples were produced for the first time in this study. The micrograph of Figure 4.13.b displayed the high magnification view of the coat layer with quite a homogeneous and smooth surface with only a small concentration of micro-porosity present. The similarity between the microstructures of Figures 4.12.d and 4.13.b was actually expected.

At this point of this study, a "working solution recipe" for successful dip-coating process has thus been obtained for the first time for the sol-gel-based dip-coating of stainless steel (316L) strips with calcium hydroxyapatite. The processing flow-chart for this solution recipe [*] was given in Figure 4.14. In this flow-chart, WIB means "water-ice bed," whereas, the numbers in the ellipsoids refer to the ultrasonic irradiation level (see Table 3.1) and the time at this level (in minutes), respectively. The solution of this flow-chart was named as **SOL2** in the rest of the text.

In the following phase of this study, the organic additive gelatine was removed from the experimental solution recipe because of the difficulties encountered in the

[*] ***Patent pending***, TPE, Ankara, January 13, 1999.

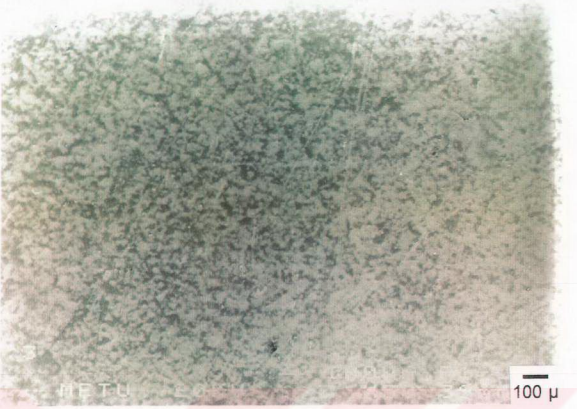

Fig. 4.13.a. SEM micrograph of sample **SS4.**

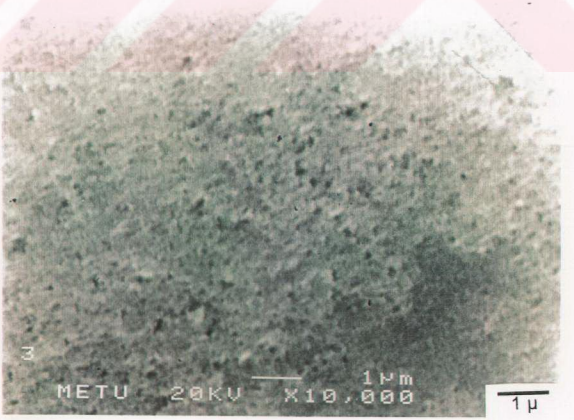

Fig. 4.13.b. SEM micrograph of sample **SS4.**

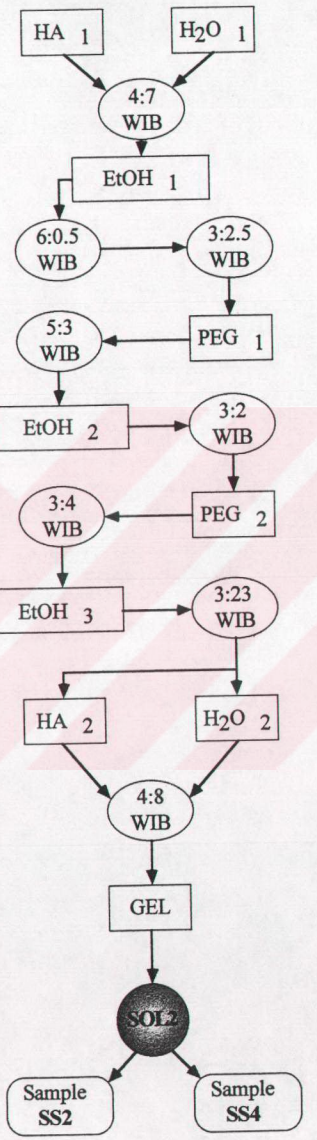

Fig. 4.14. The processing flow-chart of **SOL2**.

processing and mixing of gelatine together with ethanol and distilled water. The flow-chart of Figure 4.14 was a bit complex and hard to reproduce when needed, and for that reason another, more simplified processing route for the solutions was searched for.

The **SS5** samples were ground with a 1200-grid SiC paper in a direction perpendicular to that of dipping which was done manually. The preparation conditions and the formula of the dip-coating solution used in this series of samples were depicted as **SOL4** in Table 4.1. The **SS5** samples were heat-treated in a flowing N_2 atmosphere at 840°C in a horizontal tube furnace. The coating layers of such samples were investigated by SEM studies. The picture given in Figure 4.15 displayed the microstructure of the coat HA layer obtained on the stainless steel substrate. The microstructure was free of cracks in its entirety. This sample also proved that by the elimination of gelatine from the solution recipe, it was again possible to obtain homogeneous, smooth, crack-free coatings of HA which were also resistant to the rapid 90°C-drying in air, following the dip-coating. The solution recipe developed for this series of samples were also found to be much simpler and easier to work with. The EDXS analysis performed on the dip-coated **SS5** samples were reproduced in Figure 4.16. It exhibited a typical EDXS chart for single-phase calcium hydroxyapatite, without any peaks of the base metal.

In summary for the process of dip-coating of stainless steel samples with HA, two different recipes for solution preparation have been obtained and these were able to yield crack-free and homogeneous coatings. These solutions were labelled as **SOL2** and **SOL4** in Table 4.1.

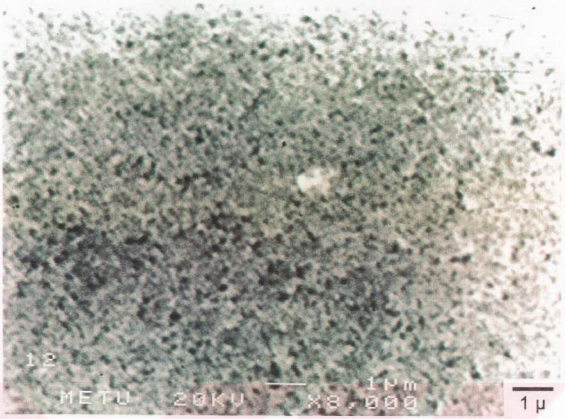

Fig. 4.15. SEM micrograph of sample **SS5**.

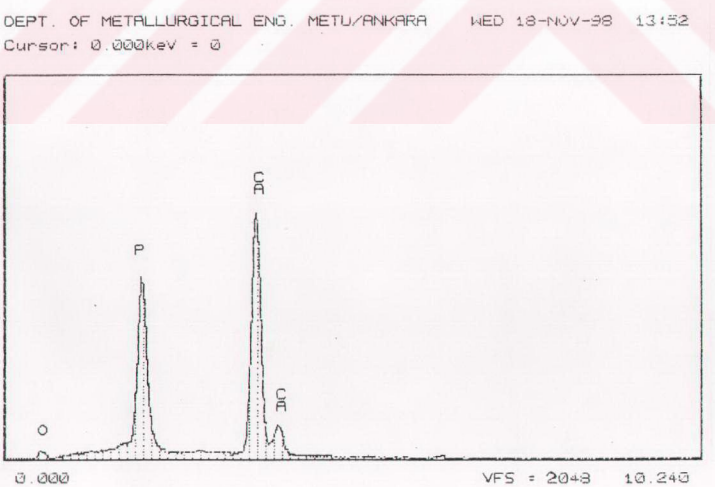

Fig. 4.16. EDXS plot of HA coating of sample **SS5**.

4.2.5. Dip-Coating of HA on Titanium Alloy (Ti-6Al-4V) Strips

The surface oxidation behavior of titanium alloy strips were first studied. The SEM micrograph given in Figure 4.9.a also had the same microstructure for the ground titanium alloy strips. The microstructure shown in Figure 4.17 belonged to a titanium alloy strip first ground with a 1200-grid SiC paper, after being heated at 840°C in an air atmosphere in a muffle furnace. It showed the totally oxidized surface structure with complete loss of the grinding scratches.

Pure titanium is dimorphic. The hexagonal α form changes to the cubic β form very slowly at about 880°C. Knowing that [35] Al is basically added to pure titanium as the stabilizer for the α–phase, and V as the stabilizer for the β–phase, Ti-6Al-4V has an $\alpha \rightarrow \beta$ transition associated with a significant volume change that may cause cracks in the substrate, the heat treatment temperature throughout this study was kept even below 880°C to avoid that problem completely.

The titanium alloy samples to be discussed in this section have been coded as **TA1** **TA2**. The samples were withdrawn with constant speeds from the dipping solutions.

The **TA1** samples were ground with a 1200-grid SiC paper in a direction parallel to that of dipping. The preparation conditions and the formula of the dip-coating solution used in this series of samples were depicted as **SOL4** in Table 4.1. The **TA1** samples were heat-treated in a flowing N_2 atmosphere at 840°C in a horizontal tube furnace. The coating layers of such samples were investigated by SEM studies. The micrograph given in Figure 4.18 showed almost the same microstructure as shown in Figure 4.15 for a stainless steel sample. This observation proved that the recipe given in **SOL4** formulation (which was developed for stainless steel substrates) also worked on titanium alloy samples.

The **TA2** samples were ground with a 1200-grid SiC paper in a direction parallel to that of dipping. The preparation conditions and the formula of the dip-coating solution used in this series of samples were depicted as **SOL5** in Table 4.1. In contrast to **SOL4** formulation used in the **TA1** samples, here gelatine was added to

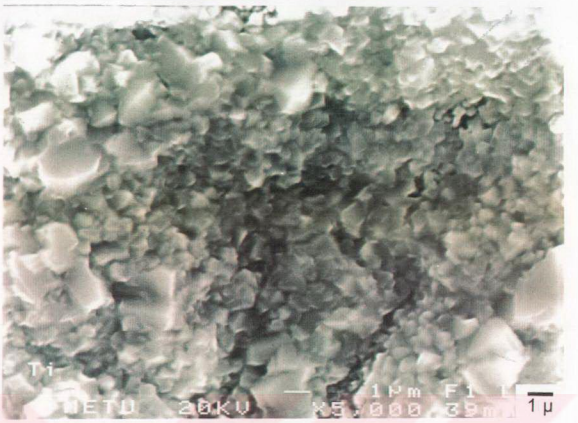

Fig. 4.17. SEM micrograph of Ti surface after heating at 840°C in air atmosphere.

Fig. 4.18. SEM micrograph of sample **TA1.**

the dip-coating solutions. The **TA2** samples were heat-treated in a flowing N_2 atmosphere at 840°C in a horizontal tube furnace. The coating layers of such samples were investigated by SEM studies.

The micrographs shown in Figures 4.19.a (low magnification) and 4.19.b (high magnification) displayed the results of a "well-working dip-coating recipe" developed for coating of an important class of orthopaedic titanium alloys. The micro-porosity observed in Figure 4.19.b is a desired property of HA-coated titanium nails and prostheses to be used in clinical implants, which would allow bone ingrowth. From the particulate nature of HA coat layer observed in this high magnification micrograph, it was apparent that the HA powders precipitated in the presence of MC possessed an average particle size of 0.25 μm after calcination at 840°C for 4 h.

The homogeneity of the coat layer-base metal interface (at the withdrawal speed of 20 mm/min), as seen in Figure 4.19.a, also proved that the dip-coating apparatus designed in this study was working properly.

The EDXS data of the **TA2** samples (Fig. 4.20) proved that the coat layer was pure calcium hydroxyapatite. The Ti peaks seen in this chart were due to the low thickness values of the coat layer as shown in Figure 4.19.b.

The experimental solution recipe* labelled as **SOL5** showed another simplification in the overall processing of several organics together with the HA powders of this study as compared to **SOL2**, flow-chart of which was given in Figure 4.14. The processing flow-chart of **SOL5** recipe was given in Figure 4.21. The recipe of **SOL4** was also included in Figure 4.21.

* ***Patent pending***, TPE, Ankara, January 13, 1999.

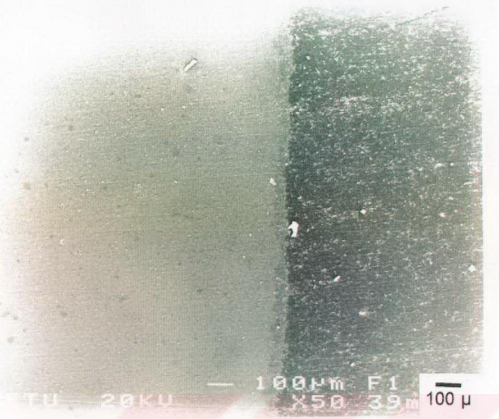

Fig. 4.19.a. SEM micrograph of sample **TA2**.

Fig. 4.19.b. SEM micrograph of sample **TA2**.

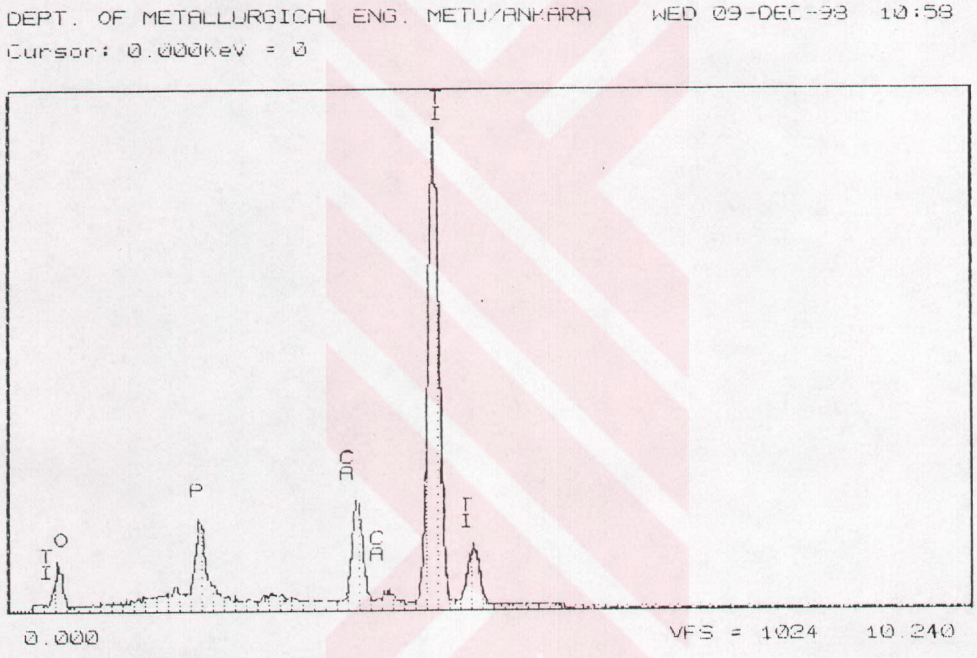

Fig. 4.20. EDXS plot of HA coating of sample **TA2**.

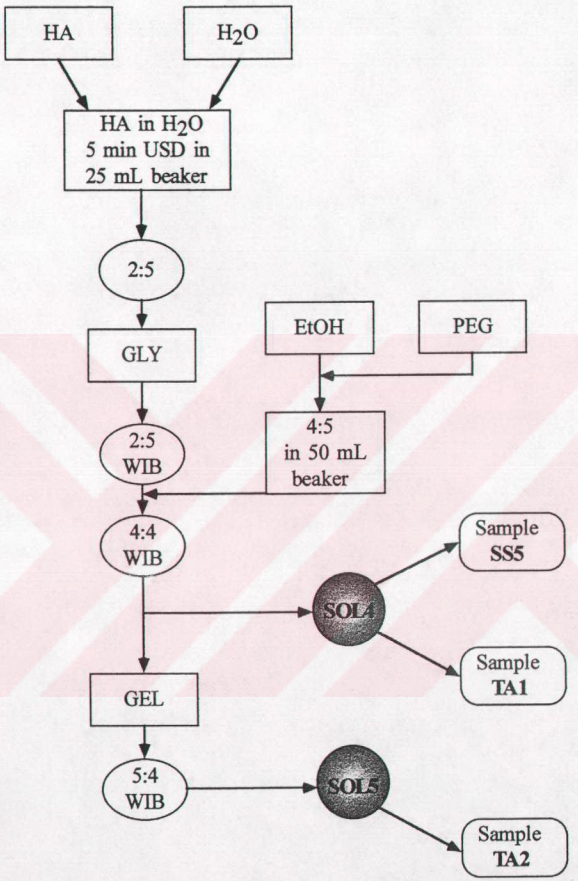

Fig. 4.21. The processing flow-charts of **SOL4** and **SOL5**.

4.3. Thickness Homogeneity in HA Dip-Coating

The SEM micrograph given in Figure 4.22 showed a highly tilted stainless steel strip dip-coated by using the solution recipe of **SOL5**. The arrows on this figure correspond to a region of 25 μm-thick. The homogeneity of the crack-free coat layer was regarded as promisingly good.

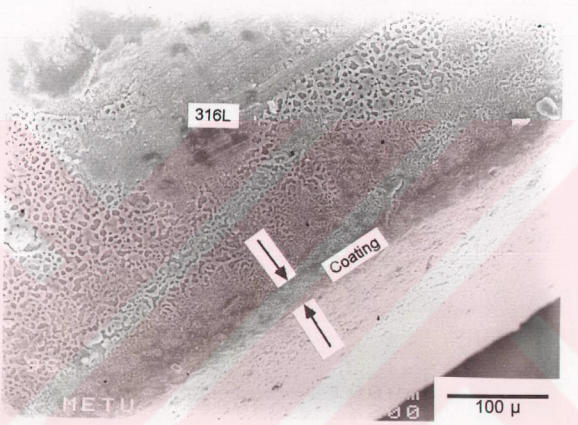

Fig. 4.22. SEM micrograph indicating the coating thickness homogeneity.

4.4. Strength of HA Coatings

Dip-coated and heat-treated samples were scratched with the tip of a screwdriver [32]. It was observed that the tip of the moving screwdriver did only made sharp scratches on the coatings without breaking apart all of the coat layer. This behavior suggested that the bulk of the coating was strongly attached to the substrate. The HA-coated metallic prostheses would only be needed to resist such low-force scratches during handling and implantation by the orthopedic surgeon.

CHAPTER 5

CONCLUSIONS

The initial addition of a small concentration of methyl cellulose to the precipitation solutions was a "*new step*" added into the aqueous chemical synthesis route [9] of HA powders. Methyl cellulose additions were performed to achieve "polymeric stabilization" in the dip-coating suspensions. The new HA powders synthesized in the present study displayed superior suspension stability in aqueous dip-coating solutions. Solutions prepared for dip-coating resisted sedimentation in a time of even several days, or in some cases, of several weeks. This has been regarded as a positive sign of the presence of "non-coagulated" and "monodispersed" sub-micron HA precipitates in the dip-coating solutions. Morphological investigations of such powders revealed that these powders had an average particle size less than 0.25 μm. The phase purity of such powders was studied by powder X-ray diffraction and EDXS. The XRD patterns of the powders which were heated over the range of 90° to 1200°C all displayed a single-phase calcium hydroxyapatite.

The metallic substrates (either Ti-6Al-4V or 316L strips) must be free of any surface contamination or surface oxide films to ensure the dip-coating of a homogeneous HA coating. Such surfaces, in the case of flat strips, can best be achieved by manual grinding with a SiC grinding paper having a grid size in the range of 800 to 1200. The effect of scratch directions placed on the strips by grinding may further be investigated. The presence of any protrusions underneath the coat layer would be the main cause of crack initiation and formation in the later stages of processing.

Dip-coating process must be performed by using a special apparatus which should

provide constant and pre-selected dipping and withdrawal rates to be variable in the range of 10 to 100 mm/min. Dipping (and withdrawal) rates are regarded to be a powerful tool in the tailoring and adjustment of coating thicknesses, as well as the HA powder concentration in the dipping solutions.

The prescription of the HA dip-coating solutions developed in the present study did not require the drying of green, coated metallic substrates under controlled humidity conditions. In other words, the coated substrates, following their withdrawal from the dip-coating solutions, had the economical advantage of being immediately and easily dried in a stagnant air oven pre-heated to 90°C, without resulting in the formation of "fast drying" cracks on their surfaces.

The calcination of the HA dip-coated metal (either Ti-6Al-4V or 316L) substrates must be performed in an inert atmosphere, such as N_2, at about 850°C. The inert gas flow rate must be no less than 4 L/min.

The organic additives in a successful dip-coating solution recipe contains the proper combinations of polyethylene glycol, glycerol, and/or gelatine in a solvent of EtOH-water mixture containing sub-micron and monodispersed powders of calcium hydroxyapatite. Two separate prescriptions for a working HA dip-coating solution have been developed and presented in this study.

The dip-coating solution recipes of the present study are shown to be able to provide a highly homogeneous and crack-free HA layer of 25 μm-thick on either Ti-6Al-4V or 316L strips, after calcination at 840°C for 4 h. The dip-coated and calcined HA layers (on top of metal strips) of this study are also found to be resistant to the well-documented "nail scratching test" applied on bioceramic-coated orthopedic implants and prostheses.

REFERENCES

[1] E. Hayek and H. Newesely, "Pentacalciummonohydroxyorthophosphate," *Inorg. Synth,* **7**, 63 (1963).

[2] E.C. Moreno, T.M. Gregory, and W.E. Brown, "Preparation and Solubility of Hydroxyapatite," *Natl. Bur. Stand.* **72A**, 773 (1968).

[3] M. Jarcho, C.H. Bolen, M.B. Thomas, J.Bobick, J.P. Kay, and R.H. Doremus, "Hydroxyapatite Synthesis and Characterization in Dense Polycrystalline Form," *J. Mat. Sci.,* **11**, 2027-2035 (1976).

[4] M. Asada, Y. Miura, A. Osaka, K. Oukami, and S. Nakamura, "Hydroxyapatite Crystal Growth on Calcium Hydroxyapatite Ceramics," *J. Mat. Sci.*, **23**, 3202-3205 (1988).

[5] C.P.A.T. Klein, J.M.A. de Blieck Hogerworst, J.G.C. Wolke, and K. de Groot, "Studies of Solubility of Different Calcium Phosphate Ceramic Particles in Vitro," *Biomaterials*, **11**, 509-512 (1990).

[6] E. Ebrahimpour, M. Johnson, C.F. Richardson, and G.H. Nancollas, "The Characterization of HA Precipitation," *J. Coll. Int. Sci.*, **159**, 158-163 (1993).

[7] S. Lazic, "Microcrystalline Hydroxyapatite Formation from Alkaline Solutions," *J. Cryst. Growth*, **147**, 147-154 (1995).

[8] A.C. Taş, F. Korkusuz, M. Timuçin, and N. Akkaş, "An Investigation of the Chemical Synthesis and High-Temperature Sintering Behavior of Calcium Hydroxyapatite (HA) and Tricalcium Phosphate (TCP) Bioceramics," *J. Mat. Sci.: Mat. in Med.*, **8**, 91-96 (1997).

[9] A.C. Taş, "Production of the Inorganic Phases [$(Ca_{10}(PO_4)_6(OH)_2$: Calcium Hydroxyapatite and $Ca_3(PO_4)_2$: Tricalcium Phosphate] of Synthetic Bones by

Using a Chemical Precipitation Technique," Patent No: TR 1995 01422 B, Turkish Patent Institute, Ankara.

[10] N. Kıvrak and A.C. Taş, "Synthesis of HA-TCP Composite Bioceramic Powders by Precipitation from Aqueous Solutions and Their Sintering Behavior," *J. Am. Ceram. Soc.*, **81**, pp. 2245-2252 (1998).

[11] L.L. Hench and J. Wilson, "*An Introduction to Bioceramics*," World Scientific, London, 1993, pp. 199-238.

[12] S.K. Ritter, "Boning Up," *Chem. Eng. News*, August 25, 27-32 (1997).

[13] S.R. Leadley, M.C. Davies, C.C. Ribeiro, M.A. Barbosa, A.J. Paul, and J.F. Watts, "Investigation of the Dissolution of the Bioceramic Hydroxyapatite in the Presence of Titanium Ions using ToF-SIMS and XPS," *Biomaterials*, **18**, 311-316 (1997).

[14] G.L. Lange and K. Donath, "Interface between Bone Tissue and Implants of Hydroxyapatite or Hydroxyapatite-coated Titanium Implants," *Biomaterials*, **10**, 121-125 (1989).

[15] M.J. Filiaggi, R.M. Pilliar, and N.A. Coombs, "Post-plasma-spraying Heat Treatment of the HA Coating/ Ti-6Al-4V Implant System," *J. Biomed. Mat. Res.*, **27**, 191-198 (1993).

[16] S.H. Maxian and J.P. Zawadsky, "Mechanical and Histological Evaluation of Amorphous Calcium Phosphate and Poorly Crystallized Hydroxyapatite Coatings on Titanium Implants," *J. Biomed. Mat. Res.*, **27**, 717-728 (1993).

[17] Y. Cao, J. Weng, J. Chen, J. Feng, Z. Yang, and X. Zhang, "Water Vapour-treated Hydroxyapatite Coatings after Plasma Spraying and Their Characteristics," *Biomaterials*, **17**, 419-424 (1996).

[18] C.Y. Yang, R.M. Lin, B.C. Wang, T.M. Lee, E. Chang, Y.S. Hang, and P.Q. Chen, "*In Vitro* and *In Vivo* Mechanical Evaluations of Plasma-sprayed Hydroxyapatite Coatings on Titanium Implants: The Effect of Coating Characteristics," *J. Biomed. Mat. Res.*, **37**, 335-345 (1997).

[19] P. Cheang and K.A. Khor, "Thermal Spraying of Hydroxyapatite (HA) Coatings: Effects of Powder Feedstock," *J. Mater. Proc. Tech.*, **48**, 429-436 (1995).

[20] M. Gottlander, C.B. Johansson, A.Wennerberg, T. Albrektsson, S. Radin, and P. Ducheyne, "Bone Tissue Reactions to an Electrophoretically Applied Calcium Phosphate Coating," *Biomaterials*, **18**, 551-557 (1997).

[21] T.M. Sridhar, T.K. Arumugam, S. Rajeswari, and M. Subbaiyan, "Electrochemical Behavior of Hydroxyapatite-coated Stainless Steel Implants," *J. Mat. Sci. Let.*, **16**, 1964-1966 (1997).

[22] K. Dijk, H.G. Schaeken, J.G.C. Wolke, and J.A. Jansen, "Influence of Annealing Temperature on RF Magnetron Sputtered Calcium Phosphate Coatings," *Biomaterials*, **17**, 405-410 (1996).

[23] M. Yoshinari, T. Hayakawa, J.G.C. Wolke, K. Nemoto, and J.A. Jansen, "Influence of Rapid Heating with Infrared Radiation on RF Magnetron-sputtered Calcium Phosphate Coatings," *J. Biomed. Mat. Res.*, **37**, 60-67 (1997).

[24] W. Yan, T. Nakamura, K. Kawanabe, S. Nishigochi, M. Oka, and T. Kokubo, "Apatite Layer-coated Titanium for Use as Bone Bonding Implants," *Biomaterials*, **18**, 1185-1190 (1997).

[25] W. Yan, T. Nakamura, M. Kobayashi, H. Kim, F. Miyaji, and T. Kobubo, "Bonding of Chemically Treated Titanium Implants to Bone," *J. Biomed. Mat. Res.*, **37**, 267-275 (1997).

[26] H.M. Kim, F. Miyaji, T. Kokubo, and T. Nakamura, "Bonding Strength of Bonelike Apatite Layer to Ti Metal Substrate." *J. Biomed. Mat. Res.*, **38**, 121-127 (1997).

[27] A.C. Taş, "Biomimetic Synthesis of Carbonated Calcium Hydroxyapatite Powders in Urea- or Urease-containing Synthetic Body Fluids," Patent Appl., January 11, 1999, Turkish Patent Institute, Ankara.

[28] A.C. Taş, "*In Situ* Coating of Calcium Hydroxyapatite on Titanium or Stainless Steel Surfaces at 37°C in Synthetic Body Fluids," 4th Ceramics

Congress, *Proc. Book, Vol. 2*, pp. 661-667, September 22-25, 1998, Eskişehir, Turkey.

[29] H.B. Wen, J.G.C. Wolke, J.R. Wijn, Q. Liu, F.Z. Cui, and K. deGroot, "Fast Precipitation of Calcium Phosphate Layers on Titanium Induced by Simple Chemical Treatments," *Biomaterials*, **18**, 1471-1478 (1997).

[30] A.P. Serro, A.C. Fernandes, B. Saramago, J. Lima, and M.A. Barbosa, "Apatite Deposition on Titanium Surfaces - The Role of Albumin Adsorption," *Biomaterials*, **18**, 963-968 (1997).

[31] M. Cabrini, A. Cigada, G. Rondelli, and B. Vicentini, "Effect of Different Surface Finishing and of Hydroxyapatite Coatings on Passive and Corrosion Current of Ti6Al4V Alloy in Simulated Physiological Solution," *Biomaterials*, **18**, 783-787 (1997).

[32] K. Ishikawa, Y. Miyamoto, M. Nagayama, and K. Asaoka, "Blast Coating Method: New Method of Coating Titanium Surface with Hydroxyapatite at Room Temperature," *J. Biomed. Mat. Res. (Appl. Biomater.)*, **38**, 129-134 (1997).

[33] S.R. Sousa and M.A. Barbosa, "The Effect of Hydroxyapatite Thickness on Metal Ion Release from Stainless Steel Substrates," *J. Mater. Sci.: Mater. in Med.*, **6**, 818-823 (1995).

[34] S.R. Sousa and M.A. Barbosa, "Effect of Hydroxyapatite Thickness on Metal Ion Release from Ti6Al4V Substrates," *Biomaterials*, **17**, 397-404 (1996).

[35] M. Long and H.J. Rack, "Titanium Alloys in Total Joint Replacement-a Materials Science Perspective," *Biomaterials*, **19**, 1621-1639 (1998).

[36] C.J. Brinker, G.C. Frye, A.J. Hurd, and C.S. Ashley, "Fundamentals Sol-gel Dip-coating," *Thin Solid Films*, **201** , 97-108 (1991).

[37] K. Kajihara, K. Nakanishi, K. Tanaka, K. Hirao, and N. Soga, "Preparation of Macroporous Titania Films by a Sol-gel Dip-coating Method from the System Containing Poly(ethylene glycol)," *J. Am. Ceram. Soc.*, **81**, 2670-76 (1998).

[38] K. Tadanaga, N. Katata, and T. Minami, "Super-water-repellent Al_2O_3 Coating Films with High Transparency," *J. Am. Ceram. Soc.*, **80**, 1040-42 (1997).

[39] S. Hirano, T. Yogo, K. Kikuta, W. Sakamoto, and H. Koganei, "Synthesis of Nd:YVO_4 Thin Films by a Sol-gel Method," *J. Am. Ceram. Soc.*, **79**, 3041-3044 (1996).

[40] Y. Ohya, H. Saiki, T. Tanaka, and Y. Takahashi, "Microstructure of TiO_2 and ZnO Films Fabricated by the Sol-gel Method," *J. Am. Ceram. Soc.*, **79**, 825-30 (1996).

[41] K. Nishio, T. Sei, and T. Tsuchiya, "Preparation and Electrical Properties of ITO Films by Dip-coating," *J. Mater. Sci.*, **31**, 1761-1766 (1996).

[42] D.B. Haddow, S. Kothari, P.F. James, R.D. Short, P.V. Hatton, and R.V. Noort, "Synthetic Implant Surfaces; *1. The Formation and Characterization of Sol-gel Titania Films*," *Biomaterials*, **17**, 501-507 (1996).

[43] D.B. Haddow, P.F. James, and R.V. Noort, "Characterization of Sol-gel Surfaces for Biomedical Applications," *J. Mater. Sci.: Mater. in Med.*, **7**, 255-260 (1996).

[44] W. Weng and J.L. Baptista, "Alkoxide Route for Preparing Hydroxyapatite and its Coatings," *Biomaterials*, **19**, 125-131 (1998).

[45] J. Carsten, P. Wange, G. Grimm, W. Götz, and W. Nisch, "Bioactive Coatings of Glass-ceramics on Metals," *Glass Sci. and Tech.*, **68**, 117-122 (1995).

[46] J. Breme, Y. Zhou, and L. Groh, "Development of a Titanium Alloy Suitable for an Optimised Coating with Hydroxyapatite," *Biomaterials*, **16**, 239-244 (1995).

[47] L. Tuantuan, J. Lee, T. Kobayashi, and H. Aoki, "Hydroxyapatite Coating by Dipping Method, and Bone Bonding Strength," *J. Mater. Sci.: Mater. in Med.*, **7**, 355-357 (1996).

[48] N. Kıvrak, "Synthesis of Hydroxyapatite (HA) / Tri-Calcium Phosphate (TCP) Composite Bioceramic Powders and Their Sintering Behavior," *M.Sc. Thesis*, METU, June 1996 (Thesis Supervisor: Dr. A. Cüneyt Taş).

[49] F. A. Şimşek, "Chemical Preparation of Calcium Hydroxyapatite (HA) in Simulated Body Fluids at 37°C and Its Use in Coating of Titanium and Stainless Steel Strips," *M.Sc. Thesis*, METU, July 1997 (Thesis Supervisor: Dr. A. Cüneyt Taş).

[50] O. Yiğiterhan, "Production of the Thin Laminates of Calcium Hydroxyapatite (HA) by Tape-Casting and Die-Pressing," *M.Sc. Thesis*, METU, January 1998 (Thesis Supervisor: Dr. A. Cüneyt Taş).

[51] N. Ö. Engin, "Manufacture of Macroporous Calcium Hydroxyapatite (HA) and Tri-Calcium Phosphate (TCP) Bioceramics," *M.Sc. Thesis*, METU, January 1999 (Thesis Supervisor: Dr. A. Cüneyt Taş).

[52] R. Moreno, "The Role of Slip Additives in Tape-Casting Technology: Part I – Solvents and Dispersants," *Am. Ceram. Soc. Bull.*, **71**, 1521-1531 (1992).

[53] C.J. Brinker, A.J. Hurd, P.R. Schunk, G.C. Frye, and C.S. Ashley, "Review of Sol-Gel Thin Film Formation," *J. Non Cryst. Solids*, **147 & 148**, 424-436 (1992).

[54] B. Maviş and A.C. Taş, "Dip-Coating of Calcium Hydroxyapatite Bioceramics on Titanium or Stainless Steel Strips," 100th Annual Meeting of the American Ceramic Society, May 3-6, 1998, Cincinnati, OH, USA, *Oral Presentation.*